

1. EXECUTIVE SUMMARY

**F. Najmabadi, R. W. Conn, N. M. Ghoniem,
R. A. Krakowski, K. R. Schultz, and C. P. C. Wong**

CONTENTS

1.1. Objectives	1-1
1.1.1. Design Goals	1-1
1.1.2. Program Approach	1-5
1.2. RFP Confinement Concept	1-5
1.3. Parametric Systems Studies	1-12
1.4. Plasma Engineering	1-14
1.4.1. Magnet Configuration	1-15
1.4.2. Plasma/Circuit Simulations	1-19
1.4.3. Current Drive	1-22
1.4.4. One-Dimensional Core-Plasma Simulations	1-23
1.5. Divertor Engineering	1-25
1.5.1. Divertor Configuration	1-25
1.5.2. Edge-Plasma Modeling	1-27
1.5.3. Divertor Target Cooling	1-28
1.6. Fusion-Power-Core Engineering	1-29
1.6.1. Self-Cooled Lithium Vanadium Design	1-32
1.6.2. Aqueous Blanket Design	1-36
1.6.3. FLiBe Pool Blanket Design	1-39
1.6.4. Helium-Cooled Ceramic Design (FISC)	1-41
1.7. Maintenance Approach	1-44
1.8. Conclusions of the Scoping Phase	1-46
1.9. Directions for the Design Phase	1-49
References	1-51

1. EXECUTIVE SUMMARY

1.1 OBJECTIVES

The TITAN research program is a multi-institutional effort to determine the potential of the Reversed-Field Pinch (RFP) magnetic fusion concept as a compact, high-power-density, and "attractive" fusion energy system from economic, environmental, and operational view-points. The primary program objectives are:

1. Determine the technical feasibility and key developmental issues of an RFP fusion reactor, especially at high power density.
2. Determine the potential economics (cost of electricity), operational, safety, and environmental features of such a high-power-density RFP reactor.

Auxiliary objectives are:

1. Establish the major technical features of an RFP reactor.
2. Develop detailed conceptual designs for the major subsystems and components.
3. Assess the degree of extrapolation between the present data base in RFP physics and in technology and the physics/technology requirements of an RFP reactor.
4. Determine the technical features and parameters of RFP devices required at key steps in a development program.
5. Develop innovative design approaches for a high mass-power-density fusion system.

Mass-power-density (MPD) is defined [1] as the ratio of net electric power to the mass of the fusion power core (FPC), which includes the plasma chamber, first wall, blanket, shield, magnets, and related structure.

1.1.1. Design Goals

Fusion reactor conceptual design has become a mature research field, and results from systems studies research have greatly influenced the direction of the physics and technology elements of the fusion energy program [2]. The

reactor studies during 1970's were focused on central power stations with electric power outputs in the range 1000 to 2000 MWe. These designs were usually based on superconducting magnets to minimize the recirculating power and generally had low neutron wall loadings ($1-2 \text{ MW/m}^2$). They shared basic disadvantages of large stored magnetic energy and FPCs, which were very large in volume and heavy in mass. These early studies projected systems with large total power output, high direct capital cost, and low power density, and generated the perception that fusion power, if feasible, would only come in units of large size and low power density and as a result would be expensive.

More recent reactor studies now seek ways to use the past experience and move toward a more affordable, competitive, and "attractive" fusion reactor. One of the approaches to the new generation of reactor design is the compact reactor option [1,3-5]. The main feature of a compact reactor is a FPC with a mass power density in excess of 100-200 kWe/tonne. The increase in mass power density is achieved by increasing the plasma power density and neutron wall loading, by reducing the size and mass of the FPC through decreasing the blanket and shield thicknesses and using resistive magnet coils, as well as by increasing the blanket energy multiplication ratio.

Even though compact designs push toward very high mass-power-density regimes, increasing realism in conceptual reactor design and costing has moved even the "conventional" designs toward smaller FPCs and higher mass-power-densities. As an example, one might begin in 1974 with UWMAK-I [8] at 20 kWe/tonne to STARFIRE [9] in 1980 and MARS [10] at 50 kWe/tonne to GENEROMAK [5] at 100-200 kWe/tonne and compact reversed-field pinch reactor, CRFPR [3,6-7] at 800-1000 kWe/tonne. A compact reactor, thus, strives toward a system with FPCs comparable in mass and volume to the heat sources of alternative fission power plants with mass power densities in the range 500-1000 kWe/tonne and competitive cost of energy. These arguments have recently prompted the suggestion that a mass power density of 100 kWe/tonne be a threshold goal for fusion reactor design [1].

Other potential benefits for compact systems can be envisioned in addition to improved economics. The FPC cost in a compact reactor is a small portion of the plant cost and, therefore, the economics of the reactor would be less sensitive to changes in the unit cost of FPC components or the plasma performance. Moreover, since a high mass-power-density FPC is smaller and cheaper, a rapid development program at lower cost is possible, changes in FPC

design would not introduce large cost penalties, and the economics of learning curves can be readily exploited throughout the plant life.

Mass power density, however, is only one general measure of the potential economic competitiveness of a fusion reactor. Other factors should also be considered in the search for an optimum fusion reactor. One can summarize the general features of an "attractive" fusion reactor as:

1. Potential for a range of power output. Reduced net power output and associated lower capital investment (investment at risk) not only makes the plant more attractive, it can also permit an affordable development pathway to bring the fusion option to commercial fruition.
2. Affordable and competitive total cost, unit direct cost (UDC, \$/kWe), and cost of electricity (COE, mills/kWeh). This goal can be achieved by:
 - A. increasing mass power density,
 - B. increasing overall plant efficiency (i.e., high thermal conversion efficiency and low recirculating power),
 - C. reducing or combining the functions of reactor subsystems and plasma support technologies.
3. Simplified overall FPC design (an obvious but usually unquantifiable operational benefit).
4. Reduced engineering constraints (e.g., magnetic fields, stresses, magnetic stored energy), simple subsystem design (e.g., large duct blanket, single coolant), and combined subsystem functions (e.g., integrated blanket/coil [11]) can lead to safe and reliable operation, reduce the forced outages, allow eased and rapid maintenance, and as a whole can drastically increase the plant availability.
5. Built-in enhanced safety and environmental features, which reduce the use of safety-specific systems and reduce the probability of accidents with either serious public health or capital cost consequences.
6. Reduced rad-waste disposal requirements. Use of low-activation materials reduces the quantity and quality of radioactive waste and eases the long term waste disposal issues.

It should be emphasized that some of these goals and features of an "attractive" fusion reactor may not be achievable simultaneously, and trade-offs are

required. The effect of these trade-offs can be assessed only through specific and detailed design.

The RFP has inherent characteristics which allow it to operate at high mass power densities (> 500 kWe/tonne). This potential is available because the main confining field in an RFP is the poloidal field, which is generated by the current flowing in the plasma. These inherent characteristics of the RFP allow it to meet, and actually far exceed, the threshold value of 100 kWe/tonne, while simultaneously meeting many of the desirable attributes for a fusion reactor, listed above. As a result, the TITAN study also seeks to find potentially significant benefits and to illuminate main drawbacks that can be obtained by operating well above the MPD threshold of 100 kWe/tonne. The program, therefore, has chosen a high neutron wall loading as the reference case in order to quantify the issue of engineering practicality of operating at high mass power density. However, the study has simultaneously put strong emphasis on safety and environmental features as well as maintainability, reliability, and availability issues. These features and constraints are incorporated into the FPC design from the beginning. For example, for the treatment of radioactive waste, TITAN aims at design concepts with 10CFR61 Class-C waste.

An important potential benefit of operating at very high mass power density is the possibility of a single-piece (or few-piece) maintenance scheme for the FPC. In such a maintenance scheme, the reactor torus is replaced as a single unit, including the plasma chamber, first wall, blanket, and possibly the shield and toroidal field coils. The potential benefits of such a replacement scheme as compared with a more "conventional" modular approach are:

1. The reactor torus is made of a few factory-fabricated pieces that are assembled on-site, in a non-nuclear environment, into a fully operational unit.
2. The FPC can undergo full operational, non-nuclear (possibly with hydrogen plasma) testing before installation in the reactor building.
3. The number of connections that must be made or broken in the nuclear environment is minimized.
4. The scheduled maintenance period is shortened because of reduced replacement time and shorter restart period with increased confidence level.
5. The procedure to recover from unscheduled events is more rapid using

more-or-less standard replacement techniques to install a stand-by and pretested torus.

6. This approach can also accommodate FPC improvement throughout the plant life and allows full benefit from learning curves economics.

These potential benefits of the single-piece maintenance approach should ultimately translate into an increase in plant availability and directly improve the economics of the plant. The TITAN study seeks to quantify and demonstrate these potential benefits.

1.1.2. Program Approach

To achieve the design objectives of the TITAN study, the program is divided into two phases, each roughly one year in length: the Scoping Phase and the Design Phase. The objectives of the scoping phase are: to define the parameter space for a high-MPD reactor; to explore a variety of approaches of major subsystems; to select at most two major design approaches consistent with high MPD; and to reach the intermediate stage of preliminary engineering design and integration. The two major approaches identified during the scoping phase would then be the subject of more detailed and in-depth analysis during the design phase.

The first half of the scoping phase was devoted to wide-range scoping studies of a large variety of different design concepts. The purpose of this period was to "let a thousand flowers bloom," and to encourage creativity and the generation of new ideas. The guidelines followed were to find concepts that held the potential to form the basis for an attractive compact RFP reactor. Those ideas and concepts that seemed promising were selected for more detailed analysis during the latter part of the scoping phase. The impact of various design options was routinely evaluated and analyzed through systems studies. At the end of the scoping phase, preconceptual design definitions of major reactor subsystems were available to initiate the design phase. This report contains the results of the scoping phase activities of the TITAN program.

1.2. RFP CONFINEMENT CONCEPT

The principles of the RFP confinement concept are summarized in this section. A more detailed description of RFP confinement is given in Ref. 12 and references contained therein.

The RFP, like the tokamak, belongs to a class of axisymmetric, toroidal confinement systems that utilize both toroidal (B_ϕ) and poloidal (B_θ) magnetic fields to confine the plasma. In the tokamak, stability is provided by a strong toroidal field ($B_\phi \gg B_\theta$) such that the safety factor exceeds unity, that is, $q > 1$, where $q(r) \equiv rB_\phi/R_T B_\theta$, and R_T and r_p are, respectively, the major and minor radii of the plasma. In the RFP, on the other hand, strong magnetic shear produced by the radially varying (and decreasing) toroidal field stabilizes the plasma with $q < 1$ and relatively modest B_ϕ . Theoretically, an electrically conducting shell surrounding the plasma is required to stabilize the long-wavelength MHD modes. In both the RFP and tokamak, equilibrium may be provided by either an externally produced vertical field, a conducting toroidal shell, or a combination of both. Figures 1.2.-1.a, b, and c respectively show, the radial variation of the poloidal and toroidal field and also the safety factor for tokamaks and RFPs.

The RFP relies strongly on the poloidal field generated by the current in the plasma. This feature has several reactor relevant advantages. The poloidal field decreases inversely with the plasma radius outside the plasma. The toroidal field is also very weak outside the plasma. The low magnetic field strength on the external conductors results in a high engineering beta (defined as the ratio of the plasma pressure to the magnetic field pressure at the magnets). Low-current-density, less-massive, resistive coils are, therefore, possible. Also, the RFP can operate at high total beta, RFPs, thereby, allowing operation at high power densities ($\propto \beta^2 B^4$). The experimentally measured poloidal beta values are in the range 10-20%, which is the range used in reactor studies. Furthermore, the RFP relies on the magnetic shear to stabilize the plasma; RFPs can, therefore, operate with a large ratio of plasma current to toroidal field, and stability constraints on the aspect ratio, R_T/r_p , are removed. High-current-density operation and ohmic heating to ignition are possible and the choice of the aspect ratio can be made solely on the basis of engineering constraints.

The fundamental property of the RFP is that the field configuration and toroidal-field reversal is the result of the relaxation of the plasma to a near-minimum-energy state, as proposed by Taylor [13-15]. These relaxed states can be described by the following dimensionless quantities: the pinch parameter, $\Theta \equiv B_\theta(r_p)/\langle B_\phi \rangle$, and the reversal parameter, $F \equiv B_\phi(r_p)/\langle B_\phi \rangle$, where $\langle B_\phi \rangle$ is the average toroidal field. The locus of relaxed states then forms a curve in $F-\Theta$ space, as is shown in Fig. 1.2.-2 (labeled as BFM). In the same figure, the

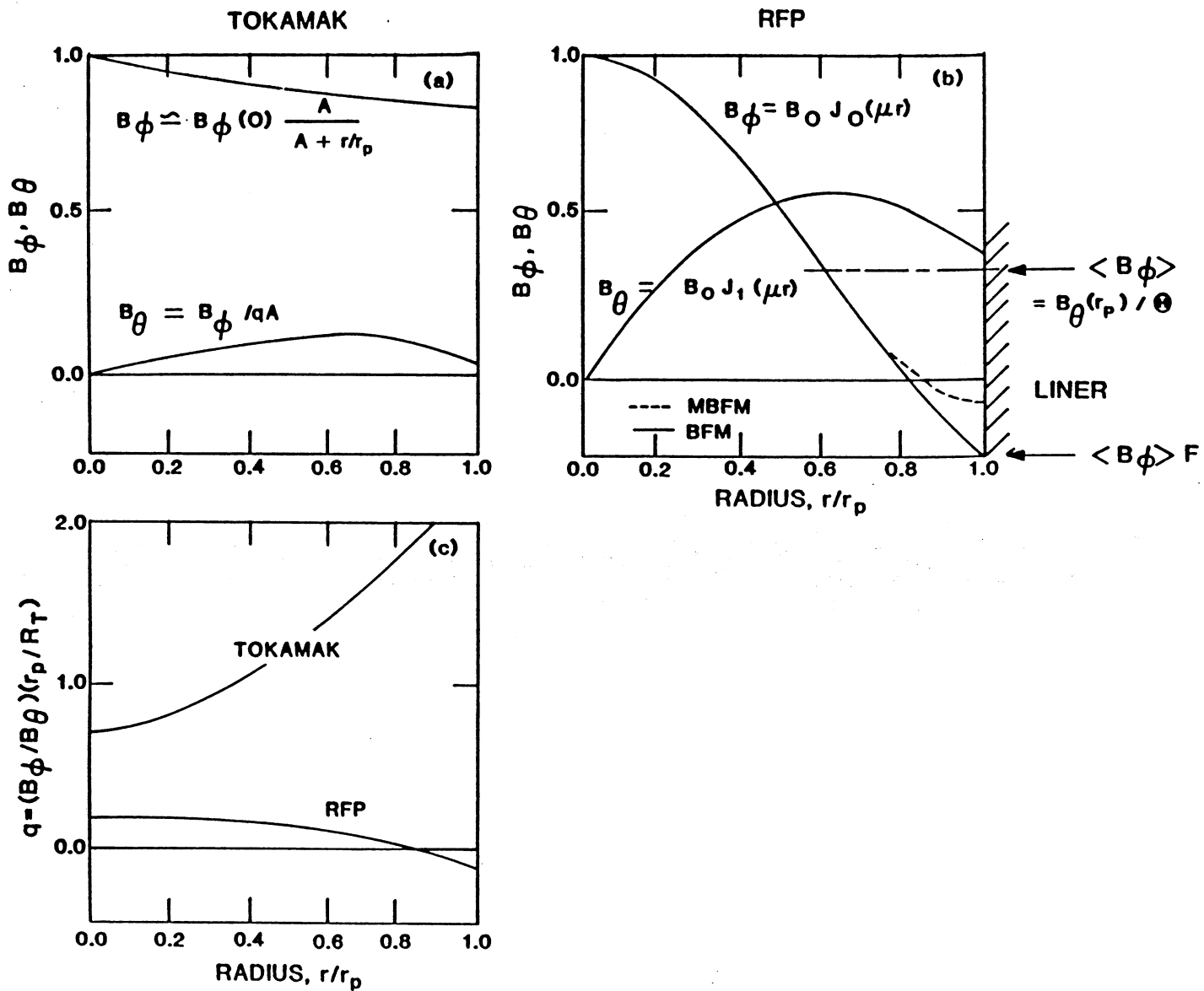


Fig. 1.2.-1. Magnetic field distribution for tokamak (a) and RFP (b) and the q profiles for tokamak and RFP (c).

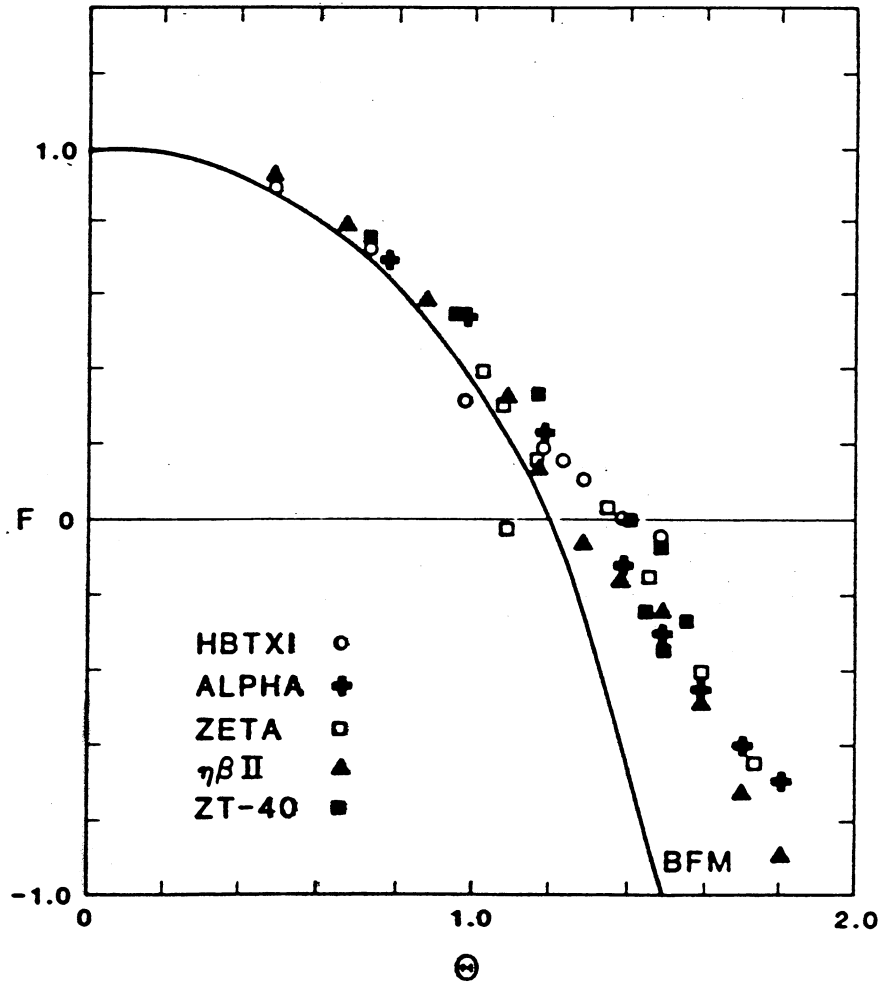


Fig. 1.2.-2. Locus of operating points on the F - Θ diagram [16]. The solid line (BFM) is the curve predicted by Taylor's theory and the data points are from several RFP experiments.

corresponding experimental data are also shown which lie to the right of Taylor's model. These experimental equilibria differ from Taylor's model since the plasma has a finite pressure, and a perfectly conducting wall is not used. The experimental points in Fig. 1.2.-2 represent "near-minimum-energy" states with finite plasma beta.

The theory of relaxed states has two important consequences. First, the theory predicts that if the current and toroidal flux are maintained constant in time (i.e., constant Θ), then the relaxed state equilibrium will be sustained. Experimentally, RFPs are observed to exist for times much larger than the decay time of the field profile due to resistive diffusion. This process involves continuous generation of toroidal field within the plasma, which compensates for the resistive decay of the toroidal field and maintains the field profile. This toroidal-flux generation process is called the RFP "dynamo".

Second, there is a strong coupling between the toroidal and poloidal fields; the toroidal field can be generated by driving toroidal current with external poloidal field circuits. This strong coupling offers the possibility of a novel and efficient steady-state current drive system through the "helicity injection" technique such as the Oscillating-Field Current Drive (OFCD) technique [17-19], which is based on low-amplitude, low-frequency oscillation of the main confining fields.

High-temperature plasmas are routinely produced in many intermediate-size RFP machines such as ETA-BETA-II in Padova [20-22], TPE-1R(M) at ETL, Sakura-Mura [23,24], ZT-40M at Los Alamos [25-27], HBTX1A at Culham [28-29], and OHTE/RFP at GA Technologies [30,31]. The plasma parameters obtained in these experiments have been improving steadily. Values of poloidal beta, β_{Θ} , in the range 0.1 to 0.2 are routinely achieved; these values are adequate for a reactor. Electron temperatures in the range 0.4-0.6 keV, densities up to about 10^{20} m^{-3} , and energy confinement times of a few tenths of millisecond are typical of these intermediate-size experiments. Data from a number of machines indicate a linear temperature-current scaling and both experimental and theoretical evidence suggests a strong scaling of $n\tau_E$ with the plasma current.

Some theoretical models for the transport in RFPs have been proposed, although a detailed transport model is not yet available for RFPs. One can use an empirical approach to evaluate present experimental results and form a basis for the extrapolation of these results to reactor regimes. Extensive measurements of the dependence of the temperature to the current indicate that the on-axis electron temperature increase with I_{ϕ} as $T_e(0) \propto I_{\phi}^{\nu'}$, where ν' is in

the range of 0.5-1.0. For several experiments, $\nu' \approx 1$ up to plasma currents of 500 kA. More recent results [32,33] suggest that the temperature-current scaling might be better described by postulating a constant beta, $nT_e(0) \propto I_\phi^2$. Evidence from a number of experiments indicates that β_θ varies relatively little over a range of conditions and from one machine to another.

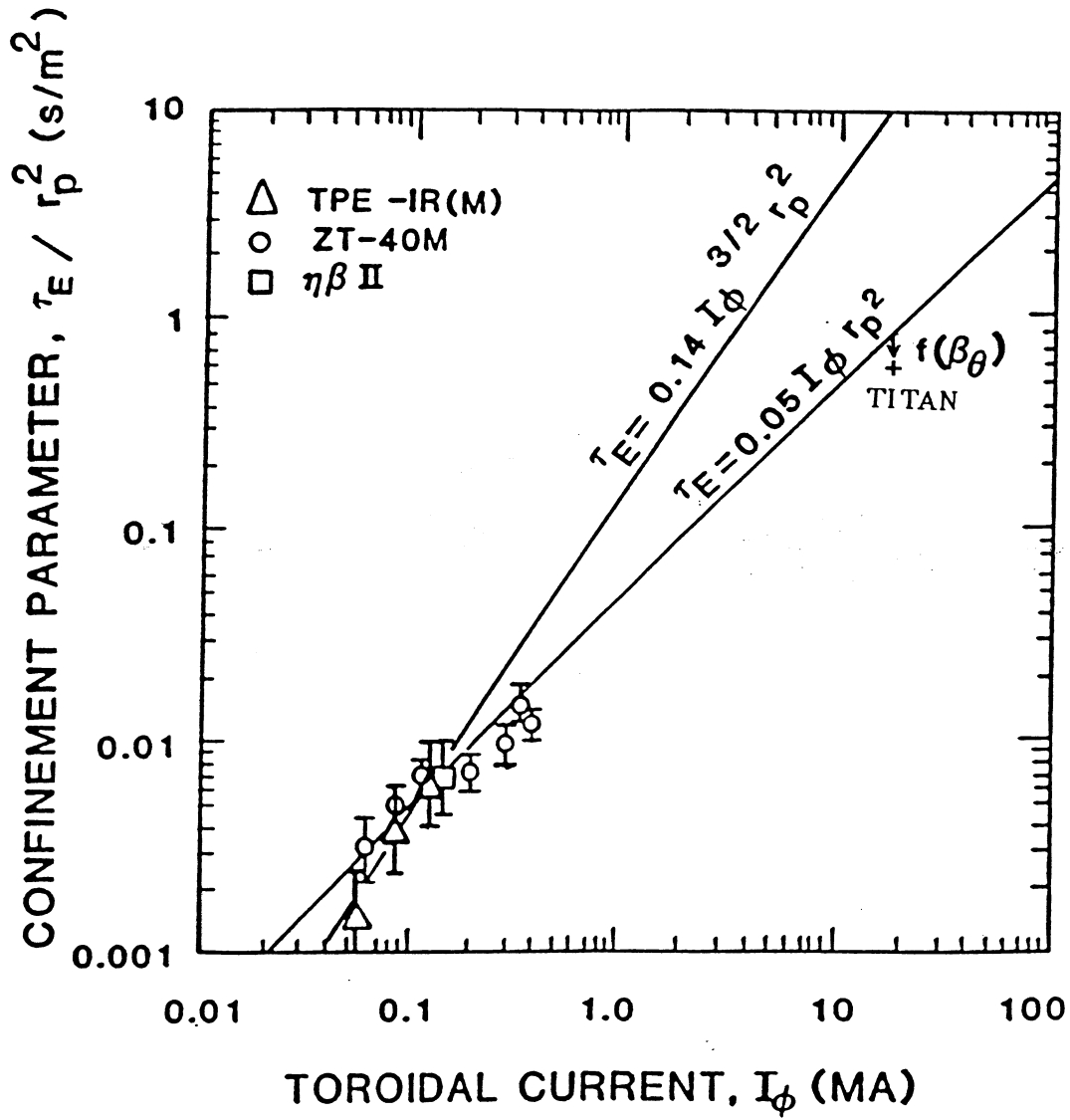
Estimates have been made of the energy confinement time, τ_E , in various RFP experiments, but only a limited amount of scaling information is available. Specifically, quantitative data on the variation of τ_E with machine radius is not available. The experimental value of τ_E is generally obtained from the ratio of plasma energy to the heating power, which is assumed to be the ohmic dissipation of the plasma current.

Under the assumptions of $T_e \propto I_\phi^{\nu'}$, the plasma electrical conductivity, $\sigma \propto T_e^{3/2}$, and $\tau_E \propto r_p^2$, the following "ohmic" scaling law can be deduced:

$$\tau_E \propto \frac{I_\phi^{5/2-\nu'}}{Z_{\text{eff}}} r_p^2 f(\beta_\theta, I_\phi/N) , \quad (1.2.-1)$$

where N is the plasma line density, and the τ_E dependence on β_θ and I_ϕ/N have been incorporated into the function $f(\beta_\theta, I_\phi/N)$. In Fig. 1.2.-3, the inverse of plasma diffusivity, $1/\chi_E \propto \tau_E/r_p^2$ is plotted as a function of I_ϕ using the data from several experiments. Two analytical curves that fit the data are also included. The design point for a RFP reactor is also shown. In the case where β_θ is approximately constant, then $T_e \propto I_\phi$ ($\nu' = 1$), and ohmic scaling Eq. (1.2.-1) yields $\tau_E \propto I_\phi^{3/2} r_p^2$ and $n\tau_E \propto I_\phi^{5/2}$, provided that Z_{eff} does not vary. A similar conclusion was also reached in OHTE/RFP where a value of $n\tau_E \sim 10^{17}$ s/m³ was recorded.

In conclusion, the theoretical and experimental data base for RFPs is less extensive than that of tokamaks and, thus, requires a larger extrapolation to reactor relevant regimes. Modern RFP experiments, however, have all demonstrated the robustness of the RFP dynamo, and a common understanding of the basic physical processes operative in RFPs is emerging. The largest uncertainties in the existing RFP data base remain in the confinement physics and, in particular, in the mechanism and magnitude of cross-field transport. Experiments with higher currents (and possibly higher current densities) and variable plasma size are needed to distinguish between different possible



scaling laws. Data from large multi-mega-ampere experiments are expected in the early 1990s [16,34]. These data are of the utmost importance in resolving some of the key physics requirements and uncertainties for an RFP reactor. Furthermore, these next-step experiments can provide valuable technological insight for devising a development path towards RFP fusion reactors.

1.3. PARAMETRIC SYSTEMS STUDIES

Parametric systems studies were performed to identify "strawman" design points and to establish the context of the design by means of sensitivity and trade-off studies. These cost-optimized strawman design points provide the starting point of a set of activities that comprises the TITAN study. First, magnetics calculations produce a realistic design for magnet coil sets needed for confinement, equilibrium, and start-up of the fusion core. Also, fusion-core plasma/circuit simulations result in detailed evaluation of key plasma parameters. These data are used to study and design the plasma support subsystems. With this detailed description of the fusion core, the engineering design activities are initiated. The neutronics, thermal-hydraulic, structural, material, and safety analyses are performed to assess the engineering performance of the key subsystems. These subsystems are then integrated into the reactor design. At each step of the analysis, feedback is provided to the systems analysis activity to improve parametric systems models which are then used to generate new, cost-optimized strawman designs for further conceptual design.

A parametric-systems-analysis (PSA) computer code is used for the sensitivity and trade-off studies. The code was originally developed for use in the CRFPR frame-work studies [2,6] and upgraded for the TITAN study. The PSA code searches for design-points with minimum COE. Parametric systems studies were performed to assess RFP reactors with a range of power outputs and neutron wall loadings, with the results shown in Fig. 1.3.-1. The dependence of COE on net plant capacity, shown in Fig. 1.3.-1, is typical of the nuclear economy of scale.

The most prominent feature of Fig. 1.3.-1 is the shallowness of the minimum of COE versus the plasma radius, r_p (and, hence, the neutron wall loading, I_w), although the compressed COE scale should be noted. This relative insensitivity is partly a result of the FPC cost being a small portion of the overall plant direct cost. In principle, other developmental and operational incentives, not

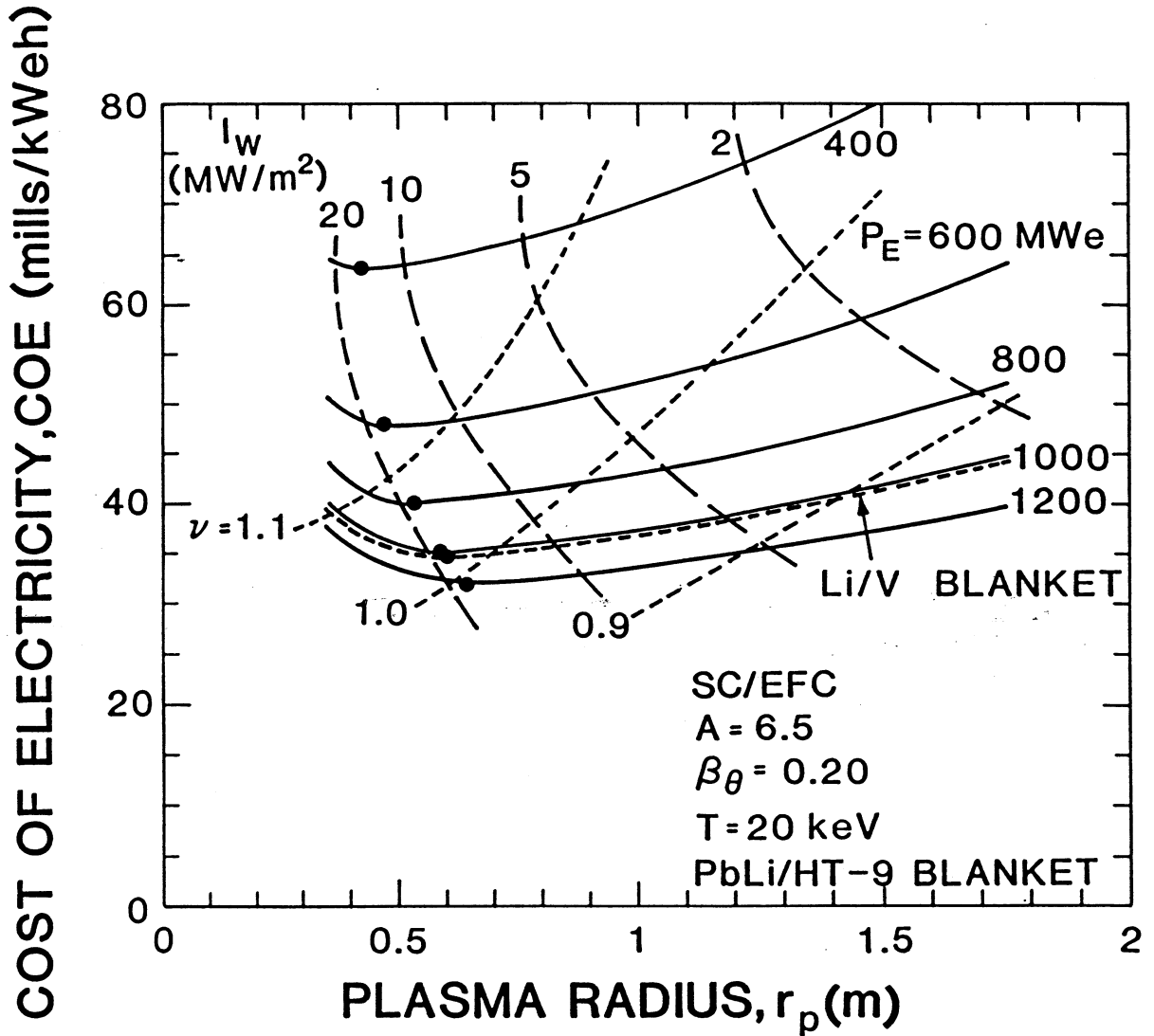


Fig. 1.3.-1. The Cost of electricity, COE, for a compact RFP reactor with PbLi/HT-9 blanket as a function of plasma radius, r_p , for a range of P_E values. The COE of a 1000 MWe RFP reactor with Li/V blanket is also shown. Contours of constant I_w as well as the condition where $\tau_E(\text{OPT}) = \tau_E(\text{PHYS})$ are shown assuming $\tau_E(\text{PHYS}) \propto I_\phi^2 r_p^2 f(\beta_\theta)$ scaling and a range of ν values.

included in the present costing model, may make the minimum of COE as a function of the wall loading more pronounced. An example is the issue of the single-piece maintenance (Sec. 1.7) and its impact on plant availability. If this approach results in a smaller plant down time compared with a modular maintenance scheme, the maximum weight and size of the FPC that can be maintained as a single-piece may introduce an abrupt change in plant availability and, hence, in COE. The TITAN study seeks to quantify potentially significant benefits or drawbacks that results from operating at very high wall loading and mass power densities well above the threshold of 100 kWe/tonne.

The CRFPR framework studies [3,4,6,7] focused on a design with a neutron wall loading of $I_w \approx 20 \text{ MW/m}^2$, high-coverage (poloidal) pump limiters, Oscillating-Field Current Drive (OFCD) for steady-state operation [17-19], and single-piece FPC maintenance. The reactor featured a water-cooled copper first wall, a self-cooled $\text{Pb}_{83}\text{Li}_{17}$ /ferritic-steel (HT-9) blanket, and thin (0.10-m) steel shielding. Also, resistive copper-alloy toroidal-field (TFC), ohmic-heating (OHC), and equilibrium-field coils (EFC) were used.

The present focus of the TITAN study is a 1000 MWe (net) reactor. Typical physics, engineering, and costing parameters are listed in Table 1.3.-I and compared with the CRFPR study. The TITAN design is a divertor-based [35], high-neutron-wall-loading ($10\text{-}20 \text{ MW/m}^2$) reactor that also invokes OFCD for steady-state operation, retaining the motivation of high power density, compact fusion. A range of pool- and loop-type blanket concepts is being considered. The TITAN design features superconducting EFCs in order to eliminate steady-state power consumption in the resistive EFC, combined with a desire for a more open FPC geometry for the ease of maintenance. The OHCs and TFCs in TITAN, however, have remained as resistive-coil systems in order to retain a compact reactor torus, with the OHC being used only for start-up. An elevation view of TITAN is shown in Fig. 1.3.-2 which illustrates the "openness" of the TITAN design for maintenance purposes.

1.4. PLASMA ENGINEERING

The plasma engineering effort starts with the TITAN "strawman" designs (Table 1.3.-I), which are generated by the parametric systems analysis. Then, magnetics calculations produce a realistic design for magnet coil sets needed for confinement, equilibrium, and start-up of the fusion core. Also, plasma/circuit simulations result in detailed evaluation of key plasma

TABLE 1.3.-I

SUMMARY AND COMPARISON OF 1000-MWe TITAN STRAWMAN DESIGN-POINT

	<u>TITAN</u>	<u>CRFPR [6]</u>
Neutron wall loading, I_w (MW/m ²)	18.	19.
First-wall minor radius, r_w (m)	0.65	0.75
Plasma minor radius, r_p (m)	0.60	0.71
Plasma major radius, R_T (m)	3.90	3.90
Average plasma density, $n(10^{20}/m^3)$	4.35	6.55
Average plasma temperature, T(keV)	20.	10.
Poloidal beta, β_θ	0.20	0.23
Plasma current, I_ϕ (MA)	17.75	18.4
Energy Confinement Time, τ_E (s)	0.27	0.23
Pinch parameter, Θ	1.55	1.55
Reversal parameter, F	-0.10	-0.12
Poloidal field at plasma surface, B_θ (T)	5.2	5.2
Reversed-toroidal field during burn, $-B_{\phi R}$ (T)	0.36	0.40
Engineering Q-value, $Q_E = 1/\epsilon$	7.84	5.0
Fusion power, P_F (MW)	2,261.	2,733.
Total thermal power, P_{TH} (MW)	2,866.	3,472.
System power density, P_{TH}/V_{FPC} (MWt/m ³)	12.8	9.7
Mass power density, $1000P_E/M_{FPC} = MPD$ (kWe/tonne)	644.	800.
Cost of electricity, COE(mills/kWeh)	35.	37.

parameters. These data are used to study and design the plasma support subsystems. As a whole, the fusion core physics activity provides a detailed description of the fusion core for all engineering activities and design efforts. Feedback is also provided to the systems analysis activity to improve parametric systems models which are then used to generate new, cost-optimized strawman designs for further conceptual engineering design.

1.4.1. Magnet Configuration

The magnet configuration consists of a poloidal-field coil (PFC) set, a toroidal-field coil (TFC) set, a divertor coil set, and an Oscillating-Field Current-Drive (OFCD) coil set. The divertor and the OFCD analyses have not progressed sufficiently to yield specific coil designs.

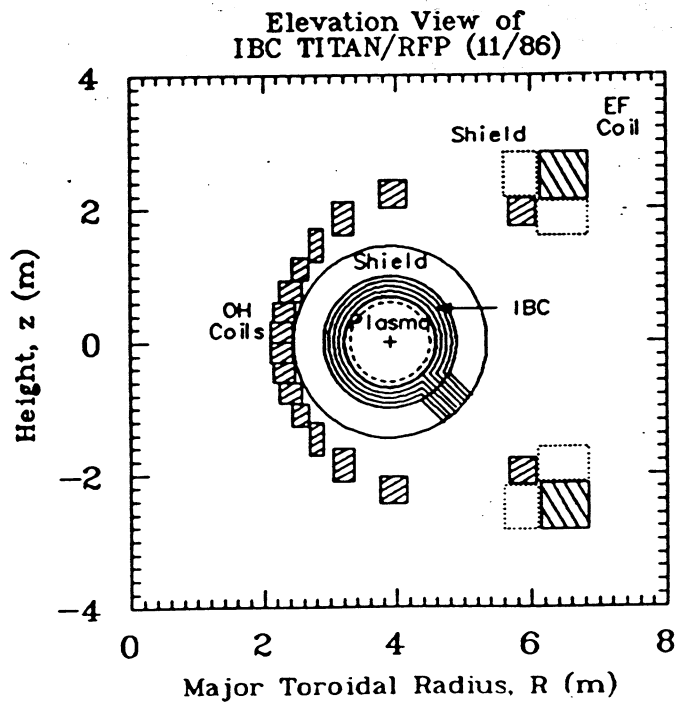
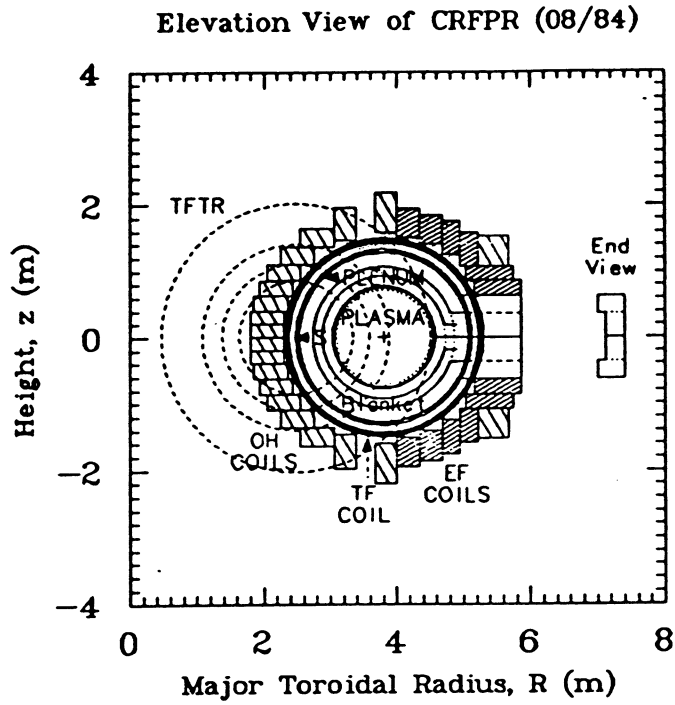


Fig. 1.3.-2. The elevation views of the TITAN reference case and CRFPR [3,6].

1.4.1.1. Poloidal-Field Coil (PFC) System

The PFC set performs both an equilibrium and an ohmic-heating (start-up) function. The equilibrium function requires that a vertical field of a certain magnitude and index, related to the plasma current and beta, be imposed over the plasma cross section in order to maintain the plasma against the outward expansive forces arising from plasma and poloidal-field pressure. The ohmic-heating function provides the poloidal-flux swing required to establish the steady-state plasma current, which is then subsequently sustained by OFCD. Since the ohmic-heating function is required only during start-up and the equilibrium function is required continuously, the PFC set is naturally, but not necessarily, split into two coil sets: an equilibrium-field coil (EFC) set and an ohmic-heating coil (OHC) set.

Equilibrium-Field Coils (EFCs). Since the EFCs are continuously active, the recirculating power can be minimized by using superconducting EFCs. Superconducting EFCs, however, require ≥ 1.5 m of blanket and shielding between the coils and plasma compared with ≤ 0.8 m for resistive EFCs; hence, more current is needed to produce the same field resulting in a more massive and expensive coil set. The trade-off between normal-conducting and superconducting EFCs was examined and found to weigh somewhat in favor of superconducting EFCs (Sec. 5.3). Consequently, the use of superconducting EFCs was adopted for this study. A more detailed analysis of the superconducting EFC performance during the plasma transients are underway. An additional constraint is imposed to use only a single pair of EFCs positioned not to interfere with vertical or horizontal movement of the first wall, blanket, shield, and TFC assembly during maintenance procedures. The PFC arrangement for TITAN is shown in Fig. 1.3.-2, which generally meets the above requirements.

Ohmic-Heating Coils (OHCs). An efficient coupling of OHCs to the plasma is obtained with the "close-fitting" OHC configuration shown in Fig. 1.3.-2. Such a configuration requires the removal of most of the OHCs in the upper-half plane to gain access to the reactor torus for (single-piece) maintenance purposes. In order to eliminate the need for coil movement for maintenance purposes, the OHCs can be arrayed into two vertical stacks with one stack positioned inboard of the torus and one positioned outboard (Fig. 4.4.-2).

The OHC set should be designed to couple efficiently with the plasma in order to minimize the start-up power and voltage requirements and the

engineering issues associated with the OHC magnet design (e.g., stresses). An additional constraint on the OHC design is the maximum level of the stray vertical field during breakdown.

Both the "close-fitting" and the "vertical-stacks" configurations were analyzed in the scoping phase. Given practical limits on start-up power and voltages, only the close-fitting configuration was found to comply with the stray-vertical-field constraint. This configuration was adopted, and a reference PFC design was produced which is shown in Fig. 1.3.-2.

1.4.1.2. Toroidal-Field Coil (TFC) System

Two options are being considered for the TFC set. The first is a resistive, copper TFC set, positioned outside the blanket and shield. In order to permit service access to the reactor torus, the TFCs must be discretized rather than forming a continuous toroidal shell. The discrete TFC set, however, introduces a toroidal-field ripple which can adversely affect the confinement. Therefore, the management of the ripple is a major factor in the design of the TFCs.

An accurate assessment of island widths can be obtained from three-dimensional field-line tracings which simulate the toroidal, radial, and poloidal components of the magnetic field. Although such simulations remain to be done for this study, previous simulations [3] indicate that islands can be kept acceptably small if $\Delta B_R/B_\theta < 0.003$, which is the criterion used for the ZT-H design [16]. Scaling the number of TFCs from that design has resulted in a preliminary TFC design with 28 TF coils.

The design issues associated with the toroidal-field ripple has led, in part, to the consideration of the integrated blanket/coil (IBC) concept [11] (Sec. 8.2.5) as a second TFC option. The IBC concept combines blanket and TFC functions by using a liquid metal, which breeds tritium to fulfill the blanket function, flows so it can remove the energy deposited within it, and conducts electricity to fulfill the TFC function. The combination of functions eliminates the need for coolant penetrations through the conductor. With the major penetrations eliminated, the TFC current channel approaches a continuous toroidal shell which in principle introduces no toroidal-field ripple. However, the IBC has a number of potential problems such as high-current (1-2 MA), low-voltage (8-10 V) power supplies, field errors produced in the vicinity of the current leads, and the trade-offs between thermal-hydraulics flow paths and electrical flow paths.

1.4.2. Plasma/Circuit Simulation

It became evident towards the end of the early RFP reactor studies [3,6] and during the earliest phase of the TITAN study that both the TFC and PFC (OHC + EFC) design limits would be determined more by the plasma breakdown, formation, and ramp-up transients than by the steady-state operational phase. Both the desire to use the RFP dynamo to generate internal toroidal flux, rather than injecting all the toroidal flux by the TFCs, and the OHC back-bias stress and power strongly influence the TFC and OHC designs. Furthermore, the PFC configuration determines the coupling of OHC with the plasma, the magnitude of the stray vertical field, and the degree of multipolarity of field nulls in the plasma chamber. These in turn influence the breakdown and RFP formation conditions through the amount of initial (vacuum) toroidal field, $B_{\phi 0}$, and ultimately affect the TFC design.

A body of experimental data is beginning to accumulate, which better defines the formation "window" and associated PFC/TFC circuit requirements for the TITAN RFP reactor. Although much of this information is not theoretically understood fully and extrapolation from ZT-40M-class experiments to a reactor is uncertain, this information and experience nevertheless is assimilated for the first time and used as part of the TITAN study. The formation phase of the RFP is characterized by the following experimentally observed behaviors:

- ♦ upper and lower density limits define a region outside of which poor or no RFP formation occurs.
- ♦ minimum plasma current (or possibly current density, in that size variations are limited in present-day experiments) below which robust RFPs cannot be formed.
- ♦ minimum limit on the toroidal electric field, E_{ϕ} , or ratio of E_{ϕ} to initial filling pressure, E_{ϕ}/P_0 , to ensure break-down.
- ♦ upper limit on the formation time, τ_R .
- ♦ limits imposed on initial (vacuum) toroidal magnetic field, $B_{\phi 0}$.

In addition to setting windows for RFP formation, relationships between these variables and the poloidal-flux and energy consumption during formation have been derived [36]. These constraints are summarized in Sec. 4.5.1 and formulated into a simplified breakdown and formation model that in turn is evaluated to provide initial conditions for the simulation of plasma start-up, ignition and burn.

An important result of the foregoing analysis is the evaluation of the impact of stray vertical field on the RFP formation requirements. Any increase in the stray vertical field produced by the OHC set at the back-bias, results in increases in the flux, energy, and power consumption during the RFP formation phase. Since the resistive poloidal-flux consumption during the full ramp-up to ignition and burn is ~ 25 Wb ($\sim 10\%$ to total), an additional flux consumption during formation much above this value becomes a concern from the viewpoint of back-bias stress in the OHCs. As a result, a maximum value of 2.5 mT for the stray vertical field was adopted for the OHC design.

Analysis of plasma circuit interactions determines the plasma response to the externally applied fields. Such analyses are required so that appropriate switching sequences and voltages can be applied to the external circuitry (e.g., PF and TF coils) for various transient plasma operations, such as start-up and shut-down, fractional power operation, and Oscillating-Field Current Drive (OFCD). This simulation is performed through a plasma/circuit interaction code. The preliminary results given for the RFP formation phase have been used to estimate initial conditions for the simulation of the post-formation fast current ramp (few seconds to $I_\phi \approx 10$ MA) followed by a slower ramp driven from the grid to ignition and burn at $I_\phi = 18$ -20 MA. Typical results of this simulation are given in Fig. 1.4.-2.

The time-varying electromagnetic fields during the plasma transients induce eddy currents in all conducting material in the vicinity of the FPC such as the first wall, liner/conducting shell, vacuum vessel, blanket, shield, structures, etc. These eddy currents retard and modify the plasma response to externally applied fields. Furthermore, these eddy currents give rise to magnetic fields affecting the plasma equilibrium, to electromagnetic forces on all conducting materials which carry the eddy currents, and to additional energy drain from the external circuits to compensate for Joule losses by eddy currents. The eddy-current modeling is, therefore, the most critical and usually the most difficult component of plasma circuit interaction analyses. To study the impact of eddy currents on the plasma response of the TITAN reactor, a stand-alone eddy-current circuit analysis code has been developed. Application of this code to the TITAN reactor start-up and transients is guiding the coil design, FPC engineering analyses, and FPC design integration effort.

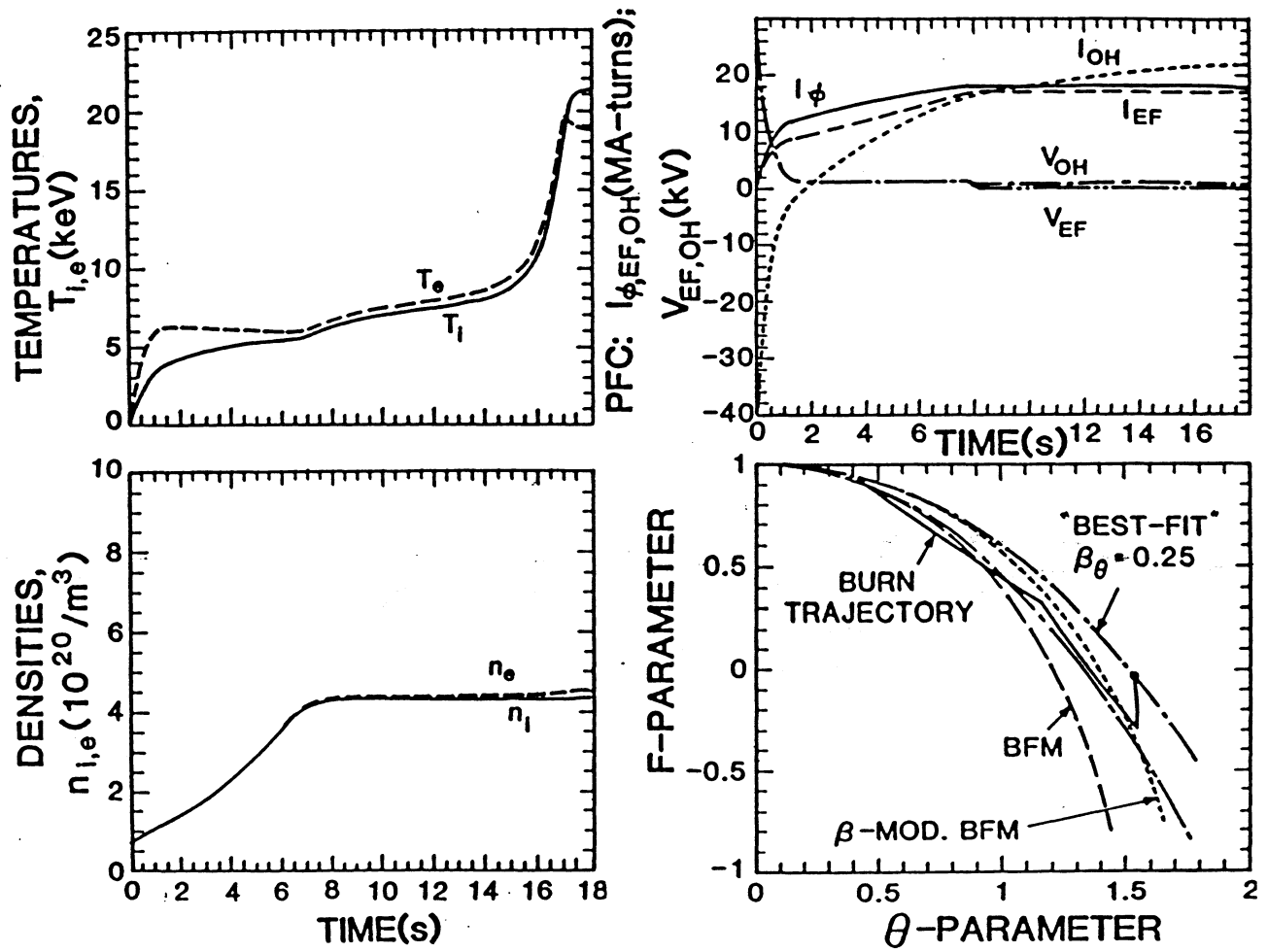


Fig. 1.4.-2. Results of a zero-dimensional plasma/circuit simulation for TITAN $I_w \approx 18 \text{ MW/m}^2$ "Strawman" design.

1.4.3. Current Drive

After considering a number of current-drive options during the scoping phase of the TITAN study, the Oscillating-Field Current Drive (OFCD) system was chosen for further evaluation. This choice was based on the projected efficiency of the drive, its relative simplicity, and the uniqueness of this scheme to the RFP.

Unlike the tokamak, the toroidal and poloidal currents in the RFP are closely coupled, since the RFP plasma profiles represent a near-minimum-energy state. If an external circuit parameter (e.g., voltage applied to TFC, V_{θ}) is varied to change the toroidal flux external to the plasma, intrinsic plasma processes related to turbulence and/or resistive instabilities generate voltages and currents within the plasma and increase or reduce poloidal flux in order to maintain the magnetic helicity constant and the plasma in a near-minimum-energy state. This nonlinear coupling between plasma and magnetic fields through the $F-\theta$ diagram, like that shown on Fig. 1.2.-2 or Fig. 1.4.-2, can be used to "rectify" current oscillations created at external coils into a net steady-state current within the plasma [17-19]. This " $F-\theta$ pumping" is envisaged to transform toroidal magnetic flux (poloidal currents) into toroidal currents (poloidal magnetic flux) through the plasma relaxation which maintains the near-minimum-energy configuration. The result is an efficient inductive but oscillatory (i.e., with no loss of electromagnetic flux) mean of steady-state current drive.

Although some experimental and theoretical basis exist, substantial current driven by OFCD has not yet been demonstrated in the laboratory and, therefore, represents a main issue for the TITAN design. Given that the OFCD principle can be fully demonstrated experimentally, the design of OFCD coils (e.g., location, sizes) and associated circuitry remains to be completed. Therefore, a plasma/circuit model for OFCD was used to identify and assess, parametrically, the potential design, power engineering, and magnetics problems. Although this model and analysis represents the first attempt to integrate circuit effects into the OFCD plasma modeling, the TITAN layout must be evolved further in other respects before a clear-cut assessment of design, power engineering, and magnetics problems can be made. This work remains for the design phase of the TITAN study. Nevertheless, the following interim observations and conclusions can be made.

The drive coils can be located outside the FPC and can probably be incorporated as a subset of windings on the main coil sets. The eddy currents induced in the material surrounding the plasma chamber distort wave-forms and

generates phase-shifts, giving rise to complications. Small plasma current swings ($\delta I_\phi / I_\phi \approx 0.02$) are sufficient to drive steady-state currents in the 18–20 MA range with resistive powers in the plasma of ~ 8 –10 MW. Large reactive power (Poynting vector) appears to flow across the plasma surface (20–30 MJ at a frequency of 60 Hz); however, the perturbation to the plasma (as measured in terms of field energy, magnetic field and current fluctuations, and fusion-power oscillations) is small. Energy flow across plasma surface (20–30 MJ) is negligible (1–2%) compared with plasma magnetic energy and is small compared with plasma kinetic energy ($\sim 10\%$). Finally, transfer occurs on a time scale (~ 60 Hz) that is 5–10% of τ_E .

The impact of the driving field oscillations on the RFP dynamo, MHD behavior, and beta remain as unresolved issues. In addition, the maintenance of plasma equilibrium during the OFCD cycle, the impact of reactive power flows on the EFC, and overall energy balance remain to be resolved.

1.4.4. One-Dimensional Core Plasma Simulations

Recent experimental evidence suggests that RFPs operate at a soft beta limit [12,16,37]. Under such a constant β_θ postulate, the transport would adjust itself by MHD activities, radiation, or any other mechanism to lose just enough energy to keep β_θ constant. In particular, f_{RAD} , the fraction of radiative power losses from the plasma to the total losses (radiation plus transport) could be controlled through impurity injection with the only penalty being a modest increase in the plasma resistance (i.e., voltage and power requirement to maintain a given current). This characteristic of the RFP soft beta limit is in marked contrast with other confinement schemes such as the tokamak, where increasing the impurity content would increase the total energy loss rate and, therefore, degrade the plasma pressure. Enhanced radiation from a (high) beta-limited plasma is important because it permits first-wall designs to receive a higher average (but more uniform) heat flux and thereby reducing the divertor (or limiter) power loads, thereby optimizing the overall design for the maximum power density while maintaining realistic engineering constraints on all systems.

Strong experimental evidence exists for a beta limit on RFPs (Sec. 4.3.6). First, a linear scaling is observed between $n_e T_e(0)$ and I_ϕ^2 for currents in the range 60–400 kA. Second, at a given plasma current level, $T_e(0)$ is found to be inversely proportional to n_e . Finally, a set of experiments was performed on ZT-40M by adding trace quantities of krypton as an impurity [16,37] to enhance

the radiative losses of the plasma. The choice of krypton was made to maximize the ratio of radiated power to the ohmic heating input. It was found that as the impurity was injected, the radiation losses were increased (with f_{RAD} as high as 95% being reported). At the same time, the ohmic input power only slightly increased, and most importantly, the poloidal beta remained constant. It follows that as radiation losses increased, the non-radiative losses decreased to preserve the constant beta.

It is important to point out that while these results are suggestive of the beta limit hypothesis, they are not conclusive. Further, it appears that far more power is being supplied to the discharge than is needed to maintain the plasma at its beta limit [16,37] and, therefore, these experiments are not expected to show the magnitude of any underlying transport which is not affected by the beta limit hypothesis.

The RFPBURN [38] one-dimensional transport model has been used to examine some of the properties of a beta-limited and radiation-dominated reactor-grade plasma. For no impurities other than a $\sim 4\%$ alpha particle ash, a minimum $f_{\text{RAD}} = 0.12$ is obtained. While low-Z impurities such as carbon can radiate the necessary power, a high impurity level is required, resulting in a high value of $Z_{\text{eff}} = 2$ for the carbon impurity, which would double the current-drive power requirements. High-Z impurities such as xenon require a much smaller impurity concentration and produce lower values of Z_{eff} (e.g., $Z_{\text{eff}}(0) = 1.3$ for Xe and the Z_{eff} decreases with radius as T_e decreases). Therefore, the high-Z impurities are favored for enhancing the plasma radiation fraction.

In conclusion, based on both experiment and theory, it is possible that RFP reactors may exhibit a soft β limit. Such a β limit was assumed in choosing the ZT-H experimental parameters [16]. If such β limits exist, it may be possible to adjust f_{RAD} to any level between 0.12 and 0.95 with only a minor increase (10-30%) in plasma resistance by injecting high-Z impurities into the plasma core. Only small variations in the impurity fraction are required to significantly vary f_{RAD} . In practice, the maximum operating f_{RAD} will be determined by the level of intrinsic transport. If the intrinsic transport mechanisms are classical, then the f_{RAD} upper limit could be higher than 0.99. Finally, it is noted that the impurity fraction of Xe required for $f_{\text{RAD}} = 1$ in the plasma core is two orders of magnitude smaller than that required for $f_{\text{RAD}} = 1$ in the divertor chamber.

1.5. DIVERTOR ENGINEERING

A considerable effort on the impurity control system has been made during the scoping phase of the TITAN study. To avoid the problems of erosion and contamination of the plasma core, associated with limiters, the use of a divertor is proposed. In choosing the type of divertor to be used, a strong preference exists for selecting a configuration in which the minority magnetic field is nulled. This choice minimizes the perturbations to the core plasma and reduces the engineering requirements in terms of coil currents, stresses, and power and energy requirements. In an RFP the toroidal field is weaker than the poloidal field at the plasma surface and bundle divertors or toroidal-field divertors are the main options, whereas a poloidal-field divertor is more appropriate for a tokamak. In the CRFPR study [6,7] it was found for the bundle divertor that the field line connection length was too long, resulting in excessive cross-field diffusion to the first wall. On the other hand, the poloidally-symmetric toroidal-field divertor was considered a feasible design approach worthy of more detailed investigation. As the reactor parameters for TITAN are similar to those of CRFPR this recommendation has been followed and the symmetric toroidal divertor has been selected as the focus of the effort on impurity control for TITAN.

1.5.1. Divertor Configuration

A typical coil layout for the divertor is shown in Fig. 1.5.-1. For TITAN the number of divertors has been set at 4 for the scoping phase, as a compromise between reducing the heat loading on the divertor target, preventing excessive Ohmic losses in the divertor coils, or paying too large a penalty on the tritium breeding ratio. The current in the central nulling coil opposes that of the toroidal field coils, while the flanking coils are present to ensure that the sum of the divertor coil currents is zero, thus minimizing the effect of the divertor on the global magnetic configuration. The field-line tracings in Fig. 1.5.-1 were obtained with a two-dimensional magnetics analysis, including the toroidal and radial components of the magnetic field. Three-dimensional modeling, which also includes the poloidal field produced by the plasma and the EFCs, is necessary to ensure that flux-surface broadening and the formation of magnetic islands because of the divertor coils do not create an unacceptable perturbation to the magnetic configuration near the plasma surface. This simulation will be performed in the design phase of the study.

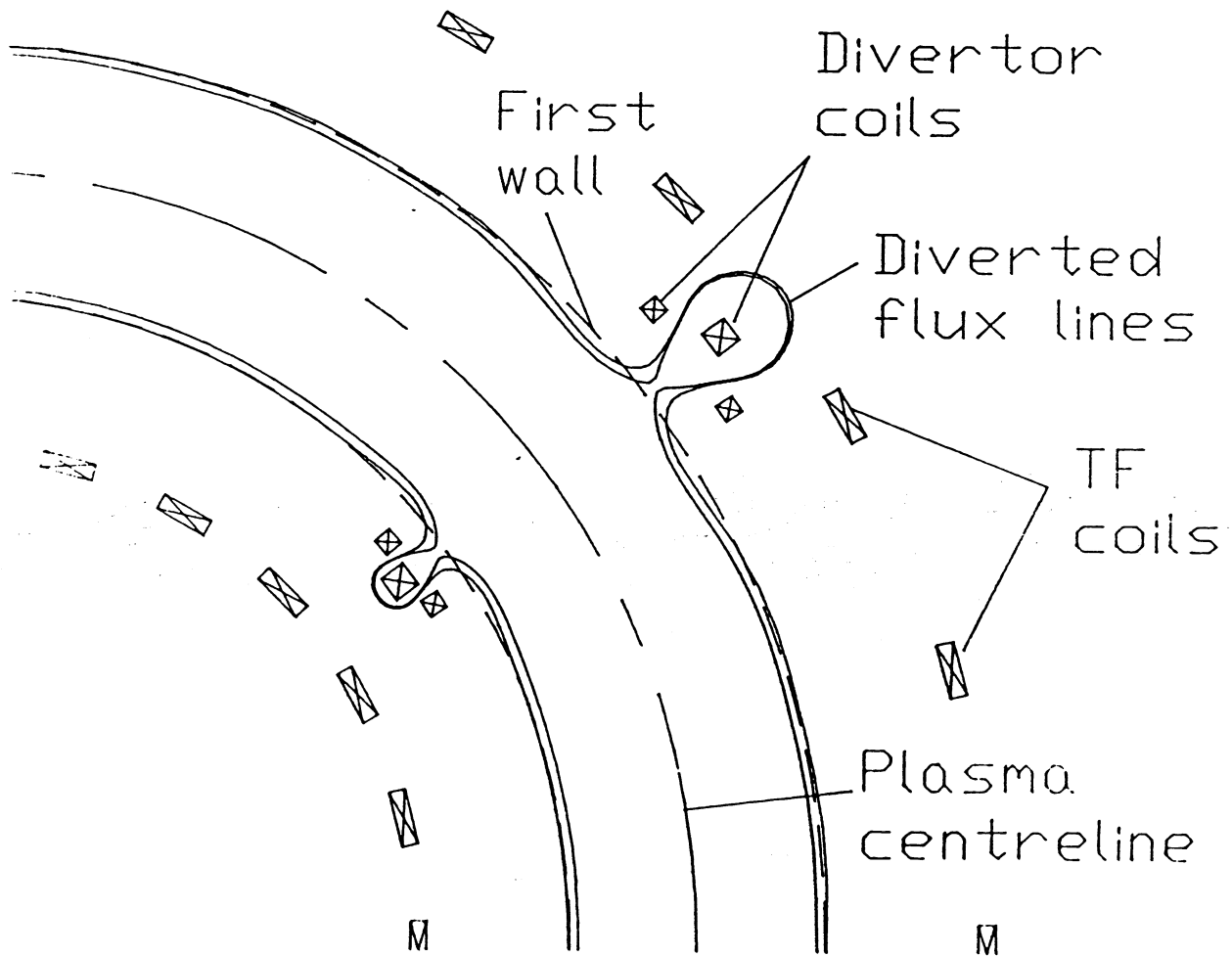


Fig. 1.5.-1. A plan view of a typical coil layout for a symmetric toroidal-field divertor showing the TF coils, divertor coils and diverted field lines on the inboard and outboard sides (generated with a 2-D magnetics analysis).

A rather closed divertor geometry is naturally obtained for the toroidal-field divertor (unlike the open geometry found with poloidal divertors in tokamak reactors), due to the proximity of the divertor coils to the plasma. This configuration allows the divertor chamber to be decoupled from the plasma chamber, and leakage or backflow from the divertor to the main plasma should, therefore, be minimal. The closed configuration also tends to cause the flux surfaces in the divertor to be compressed, increasing the heat load on the divertor plate. A more open divertor configuration is under study which seems to expand the flux surfaces in the divertor chamber, thereby reducing the heat load on the divertor plate as compared with the closed-divertor configuration.

The Integrated-Blanket-Coil (IBC) [11] approach has been considered for the divertor of the liquid-metal-cooled blanket design, which provides several advantages over a divertor design with conventional copper coils. The main benefit is that the reduction in the tritium breeding ratio and energy multiplication factor is less severe because of the greater blanket coverage obtained. A further advantage is that the coils can be located closer to the plasma, as radiation damage to the conductor and insulator poses less of a problem than for a copper coil design. The coil currents are thereby reduced, offsetting the tendency toward higher Ohmic losses caused by the high electrical resistivity of liquid lithium.

1.5.2. Edge-Plasma Modeling

Both analytic models and one-dimensional radial transport codes have been used to model the TITAN edge-plasma. These models indicate that the scale length for the radial decay of power flow in the scrape-off layer will be small, ~ 1 cm, implying that the power loads on the divertor target will be high. In an effort to reduce the heat flux to acceptable levels, the injection of high Z impurities into the divertor plasma to radiate the incident power over a wider area has been examined. A simplified analytic model has been used to show that impurity fractions on the order of a few per cent are necessary to radiate a large fraction of the power transported to the divertor. To avoid contamination of the plasma core these impurities must be efficiently confined within the divertor chamber. A criterion for the entrainment of impurities in the background plasma flow [39] has been applied to the divertor plasma but preliminary results suggest that it will be difficult to ensure that adequate retention of the impurities will be obtained.

In the design phase of the study the feasibility of confining the injected impurities in the divertor plasma will be examined with more detailed models of the edge-plasma. These improved models will allow the flows in the scrape-off layer to be studied and enable more accurate predictions of plasma parameters at the first wall and divertor target to be made, including estimates of the erosion rate due to sputtering. Improved neutral particle models will be incorporated to simulate recycling in the divertor. The core and edge-plasma models will be coupled to ensure self-consistency of heat and particle fluxes.

1.5.3. Divertor Target Cooling

Several cooling options for the divertor have been examined. Liquid metal cooling is attractive for the Li/Li/V blanket design because of its compatibility with the overall thermal cycle. For the closed-divertor configuration, the component of the magnetic field perpendicular to the coolant flow path is rather strong (~ 1 T compared with ~ 0.4 T for the first wall tubes), which limits the coolant velocity because of large MHD pressure drop. If the coolant tube walls are not electrically insulated, then the maximum wall temperature limit for vanadium restricts the acceptable heat flux to about 3 MW/m^2 for tube walls of 1 mm thickness. If insulated tube walls are used together with a coolant velocity high enough to enter the turbulent regime, heat loads of up to 9 MW/m^2 can be accommodated. For the open-divertor configuration, the perpendicular field strength is much smaller (a few tenths of a Tesla) and, therefore, the maximum acceptable heat flux for this configuration is estimated at about $6\text{--}8 \text{ MW/m}^2$.

Water-cooling is a natural choice for high-heat-flux components, although safety considerations prohibit its use in conjunction with the lithium-cooled blanket design. To maximize the heat-removal capability, the use of swirl flow in the forced convection sub-cooled boiling heat transfer regime has been considered. Copper alloy coolant tubes (of 1 mm wall thickness) allow a heat flux of about 20 MW/m^2 before the maximum allowable temperature limit is encountered for water cooling.

Helium cooling of the divertor is compatible with any of the blanket concepts considered. The very high temperature capability of SiC allows heat fluxes of up to 10 MW/m^2 to be attained for wall thicknesses of 1 mm. Similar heat loads can be accommodated with vanadium, although the coolant outlet temperature is lower. Copper has a higher thermal conductivity, suggesting its use if thicker walls are required. However, because of the lower temperature

limit of copper alloys compared with vanadium or SiC, the heat is not removed at temperatures of interest for power generation.

A brief investigation of innovative concepts has been made. Spreading the heat load by vaporization and remote condensation of a liquid metal has been shown to be not feasible because of the resulting high pressure of the vaporized material. The use of a cloud of lithium droplets to intercept the divertor plasma may be possible but the droplet must have a high velocity to reduce its temperature rise.

As the divertor design for TITAN progresses, and the expected loadings on the divertor are better defined, more detailed calculations on the thermal hydraulics and stress analysis of the divertor cooling will be made.

1.6. FUSION-POWER-CORE ENGINEERING

During the first half of the scoping phase, the TITAN design team members were encouraged to participate in a period of "concept brainstorming," and a very large number of ideas were put forward. Several of these first-wall, blanket, and shield concepts were sufficiently attractive in the context of high power density to warrant detail consideration during the scoping phase. These design concepts can be loosely categorized by the general FPC design as loop-type, pool-type, and loop-in-pool.

The loop-type concept has coolant flow in "loops" around the plasma chamber. The major feature of the loop is the efficient removal of thermal power and the ability to handle high surface heat loads. In the pool-type configuration the plasma chamber and first wall are submerged in a pool of coolant. This configuration is in principle simple, since the pool acts as a replenishable blanket and shield. Furthermore, the pool design promises the potential for inherent safety due to the large heat capacity of the pool. The major disadvantage of the pool concept is the difficult and uncertain flow configuration, which limits the high-heat-flux capabilities of the first-wall and divertor design. The loop-in-pool concept is the synthesis of several attractive ideas. The large heat capacity of the pool-type reactor promises a passively safe reactor with limits on the heat-flux capabilities of the first wall. The loop-in-pool concept submerges a loop-type first wall and blanket in a pool which acts as a heat sink during off-normal events.

The various coolant, breeder and structure options considered for the TITAN FPC are summarized in Table 1.6.-I. Following the initial period of the scoping

TABLE 1.6.-I
FPC CONCEPTS CONSIDERED FOR TITAN

LOOP-TYPE CONCEPTS

Li/Li/V: Adaptation of the BCSS [40] Li/Li/V concept to the RFP. Weak toroidal field of the RFP confinement eases the MHD effects compared with tokamaks. This concept offers the promise of high wall load, good thermal efficiency, good TBR and simple configuration. A modification of this concept is to employ the Integrated Blanket Coil (IBC) concept [11]. The IBC concept uses the blanket lithium as an electrical conductor to provide the toroidal field requirements of the RFP. External power supplies are attached to the blanket coolant headers. The IBC simplifies the FPC design by eliminating the separate TF coils and the shielding required.

He Cooled, Direct Cycle: High temperature, low activation materials are used (e.g., SiC or C/C composites) as the structure. Low activation and low afterheat could lead to an inherently safe FPC design.

PbLi: Thermal-hydraulic limitations require operation at reduced wall load or a dual media cooling system (see below).

H₂O/PbLi: This dual media design has been studied in earlier RFP designs [3,6] and offers the advantage of good first-wall cooling at high heat loads and good neutron energy recovery. Two entirely separate cooling loops are required and the reactivity between water and PbLi is a safety concern.

H₂O/K: In this dual media design, water is used to cool the first wall, but potassium is the blanket coolant. Lithium or lithium-bearing compounds, encased in metal cladding would breed tritium. The potassium would boil within the blanket and be used in a direct cycle, gas turbine. The reactivity of the water with potassium interaction is a safety concern.

TABLE 1.6.-I (continued)
FPC CONCEPTS CONSIDERED FOR TITAN

POOL-TYPE CONCEPTS

Liquid-Metal Pool: Similar concept to the French Phénix and Superphénix LMFBRs. Eddy currents produced in the pool will interfere with plasma transient operations and would require resistive baffles in the pool. Such a modification would also inhibit free coolant flow in the pool and reduce the attractiveness of this design.

FLiBe Pool: High-temperature and low-pressure operation are possible. The low electrical conductivity of FLiBe also reduces MHD and eddy current problems.

Water Pool: High pressure operation is necessary and, because of the size of the pool containment, a massive structure is required.

LOOP-IN-POOL CONCEPT

Aqueous Blanket: Lithium bearing salts (e.g., LiNO_2 , LiNO_3) are dissolved in water and used in a high pressure loop for cooling the FPC. The entire primary loop is submerged in a low pressure pool of pure water. The water pool acts as a heat sink in the event of a primary loop rupture. Beryllium is required to achieve adequate tritium breeding ratio, TBR.

phase, four FPC designs were selected for detailed engineering analysis. The final four designs are:

1. A self-cooled, lithium loop with a vanadium-alloy structure.
2. An aqueous, self-cooled design with a copper-alloy first wall, beryllium neutron multiplier and PCA structure.
3. A self-cooled FLiBe pool using a vanadium alloy structure.

4. A helium-cooled ceramic design using silicon carbide as the structure and a solid breeder.

1.6.1. Self-cooled Lithium Vanadium Design

The self-cooled, lithium loop is an adaptation of the BCSS [40] Li/Li/V design for a tokamak or tandem mirror first wall and blanket. BCSS rated this concept as the top prospect. The TITAN version of this design is illustrated in Fig. 1.6.-1 which shows the poloidal cross section and an isometric view. The isometric view shows a single quadrant of which four would be attached to form the torus. Between each quadrant would be a divertor occupying $\sim 10^\circ$ toroidally. The reactor design characteristics are given in Table 1.6.-II. The first wall of this design is made of 1.05 cm diameter tubes of the vanadium alloy, V-3Ti-1Si. The flow in these tube is poloidal, which is parallel to the stronger, poloidal field.

Because the flow is normal to the toroidal field ($B_\phi = 0.39T$), MHD effects must be considered. Analysis has shown that with high velocity lithium cooling, the first wall can handle surface heat fluxes in the range of 4 to 5 MW/m². The

TABLE 1.6.-II
OPERATING PARAMETERS FOR THE LITHIUM DESIGN

FIRST WALL

Description: Bank of lithium-cooled, seamless circular tubes;
poloidal single pass flow; inter-tube welds for
toroidal electrical circuit and to reduce fretting.

Structural material	V-3Ti-1Si
Tube o.d. (mm)	10.5
Tube i.d. (mm)	8.0
Erosion allowance (mm)	0.25
Design lifetime (full power year, FPY)	1.
Poloidal radius (m)	0.68
Number of tubes	2,440.
First wall area (m ²)	166.
Surface heat flux, peak (MW/m ²)	4.7
Volumetric heat generation (MW/m ³)	
- Lithium	76.
- Vanadium	107.
Inlet temperature (°C)	300.
Outlet temperature (°C)	393.
Mass flow rate (kg/s)	1,460.
Volume flow rate (m ³ /s)	3.08
Velocity, peak (m/s)	22.5
Pressure drop (MPa)	11.2

TABLE 1.6.-II (cont.)
OPERATING PARAMETERS FOR THE LITHIUM Design

BLANKET

Description: 4 rows of varying cross section, seamless tubes increased structural fraction with depth into blanket to maximize shield lifetime.

Structural material	V-3Ti-1Si
Tube o.d. (mm)	75.
Tube wall thickness (mm)	
- Row 1	2.75
- Row 2	3.25
- Row 3	4.00
- Row 4	4.50
Blanket thickness (m)	0.30
Volume fractions,	
- Lithium	0.64
- Vanadium	0.14
- Void	0.22
Volumetric heat generation, peak (MW/m ³)	
- Lithium	65.
- Vanadium	102.
Inlet temperature (°C)	300.
Outlet temperature (°C)	681.
Mass flow rate (kg/s)	667.
Volumetric flow rate (m ³ /s)	1.4
Velocity, peak (m/s)	0.3
Pressure drop (MPa)	1.2

SHIELD

Description: Lithium cooled, 2-piece hot shield; double-pass poloidal flow.

Structural material	V-3Ti-1Si
Moderator/absorber	HT-9
Volume fractions	
- Lithium	0.445
- Vanadium	0.044
- HT-9	0.511
Lifetime (dpa)	200.-250.
Damage rate, peak (dpa/FPY)	47.2
Inlet temperature (°C)	300.
Outlet temperature (°C)	681.
Mass flow rate (kg/s)	667.
Volumetric flow rate (m ³ /s)	1.4

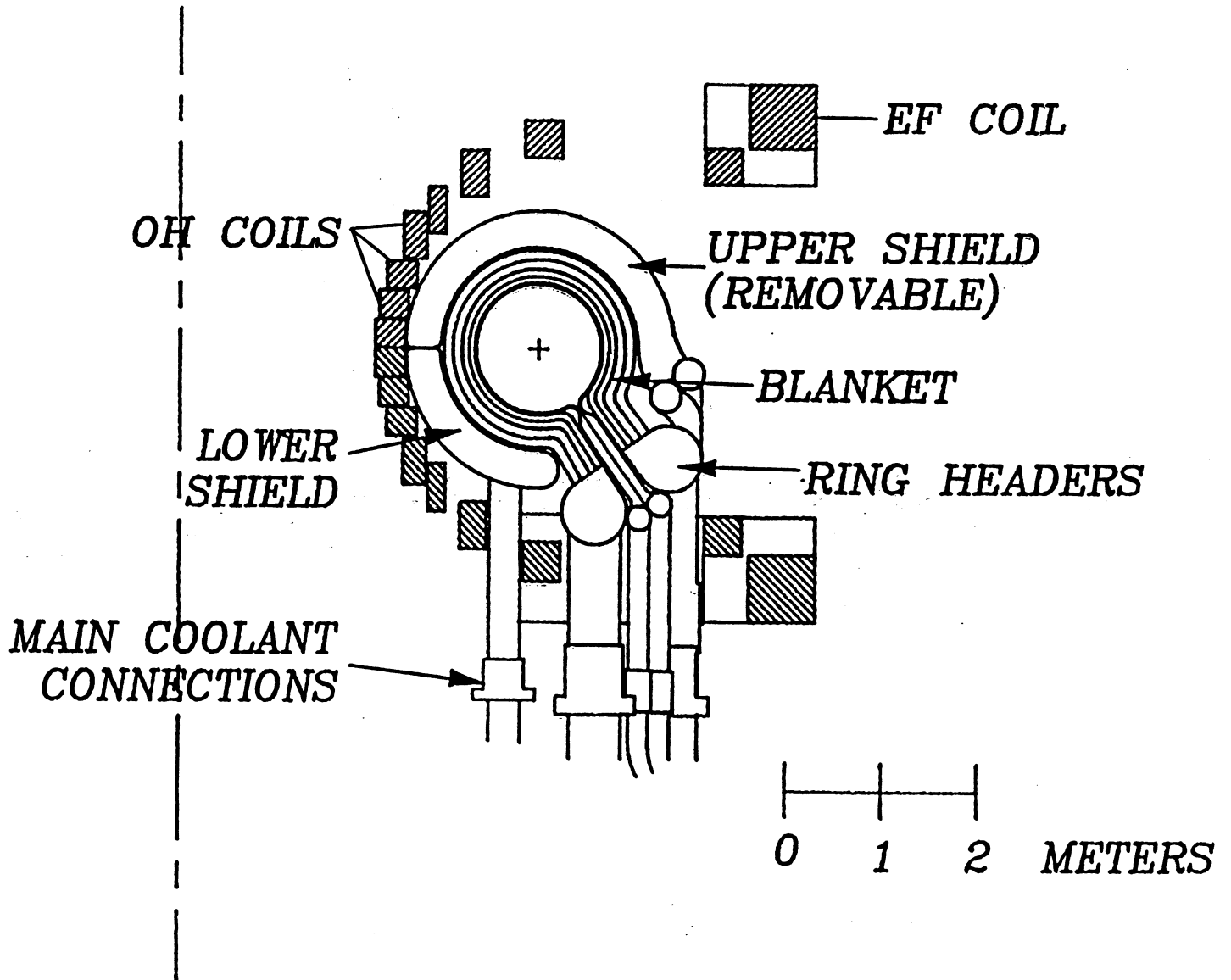


Fig. 1.6.-1a. The poloidal cross section of the Lithium design.

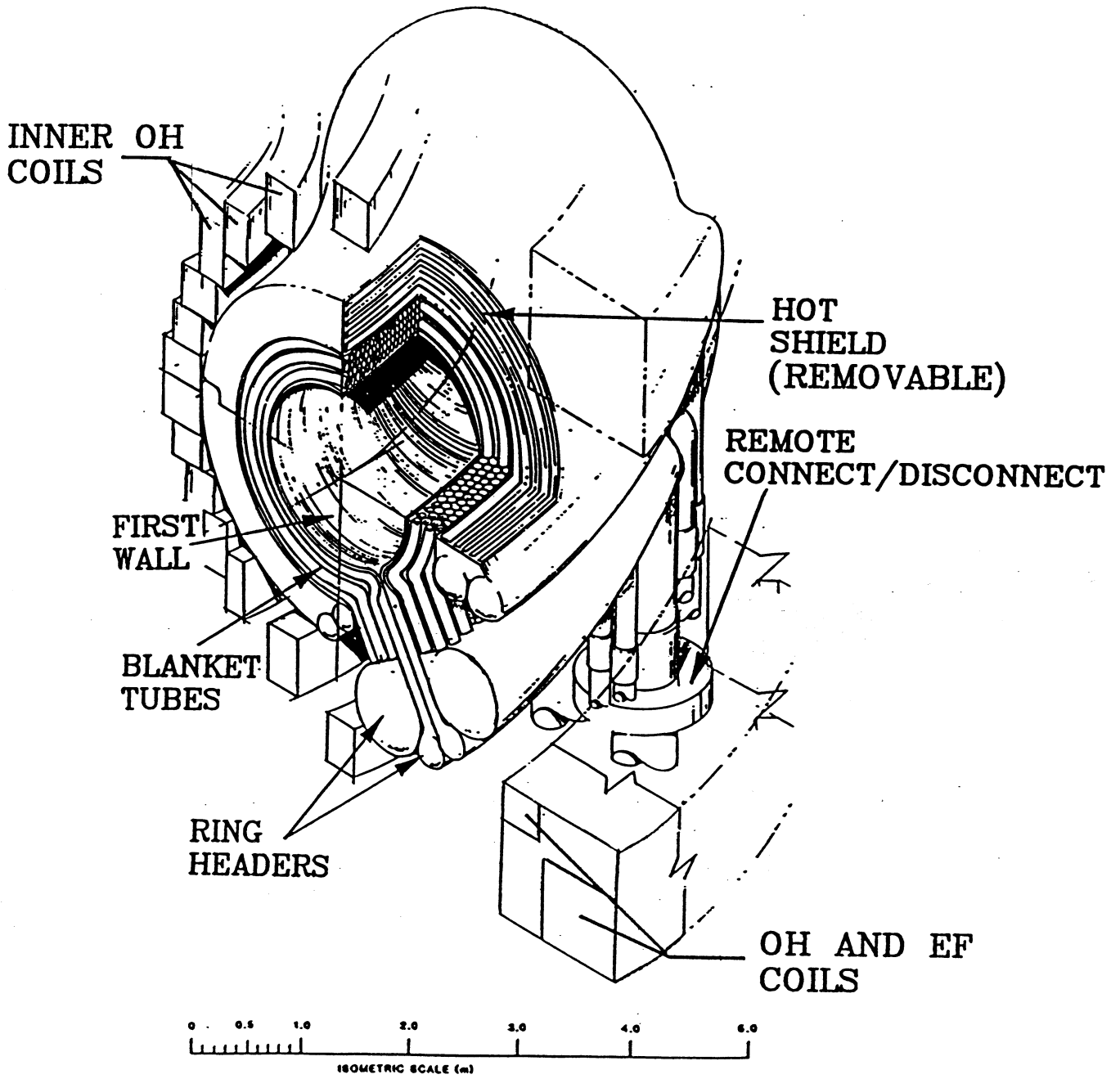


Fig. 1.6.-1b. Isometric view of one quadrant of the Lithium design.

blanket design consists of a bank of vanadium pipes with poloidal lithium flow. The blanket pipes are stacked to form a ~ 30 cm thick blanket. The shield is also lithium cooled with a vanadium structure and HT-9 neutron moderator/reflector/absorber. The shield operates at a high temperature since ~ 40% of the thermal energy is deposited within it.

The neutronics performance of the Lithium design is quite good, with a tritium breeding ratio, TBR > 1.2 and a blanket energy multiplication ratio, M ~ 1.2. Further neutronics optimization will continue during the design phase and it is expected that the neutronics performance can be enhanced. Specific areas of optimization include; thinner blanket/shield, higher M and reduced rad-waste volume.

Cooling the first wall in a high power density device is a key issue in the FPC design. As previously stated, the lithium cooled first wall is viable with surface heating as high as 5 MW/m^2 . High velocity flow is required, leading to a small temperature rise in the first wall coolant. This small temperature rise is offset by a large ΔT in the blanket and shield coolant streams. The temperature of the mixed lithium is about $600 \text{ }^\circ\text{C}$. The gross thermal efficiency of the steam cycle is about 40%.

1.6.2. Aqueous Blanket Design

The aqueous "loop-in-pool" design is the extension of the design proposed by Steiner [41], in which a high pressure primary loop including the RFP torus and heat exchangers, operating at 15.8 MPa, is submerged in a pool of water at 0.1 MPa. The general arrangement of the reactor are shown in Fig. 1.6.-2. The design characteristics of this concept are given in Table 1.6.-III.

To breed tritium, a lithium compound (e.g., LiNO_2 or LiNO_3) is dissolved in the hot water loop. The water enters the bottom of the torus at $291 \text{ }^\circ\text{C}$ and exits at the top at $326 \text{ }^\circ\text{C}$. A large number of lithium bearing salts were considered, but many resulted in solutions that were either too alkaline or had induced radioactivity problems. The nitrate and nitrite salts are the most promising, with a resulting pH of between 7 and 7.25 and a high solubility limit of between 4.5 and 6.4 a/o. High solubility is required to attain high TBR and even at the maximum lithium concentration a neutron multiplier is still required.

The water-cooled copper-alloy first wall is ideally suited for the high heat flux environment encountered in high power density devices. Subcooled flow boiling will adequately cool the first wall with 5 MW/m^2 heat flux ($f_{\text{RAD}} = 1$ for

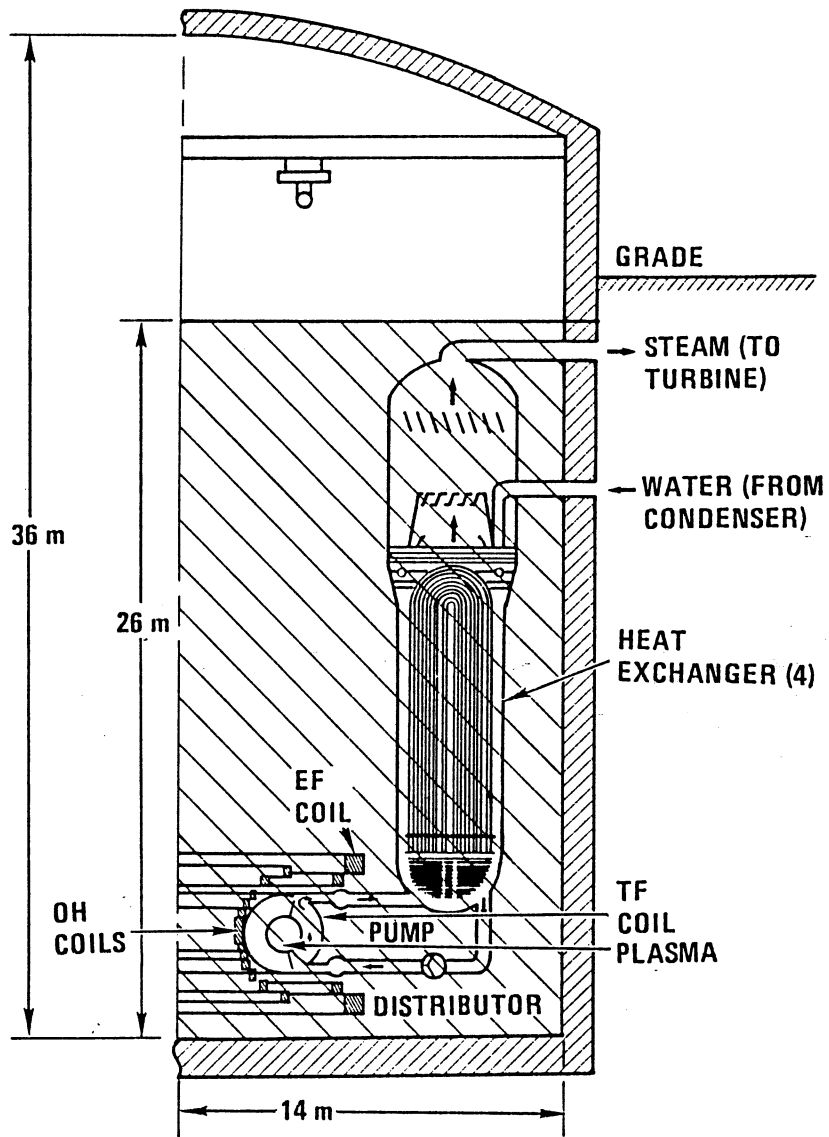
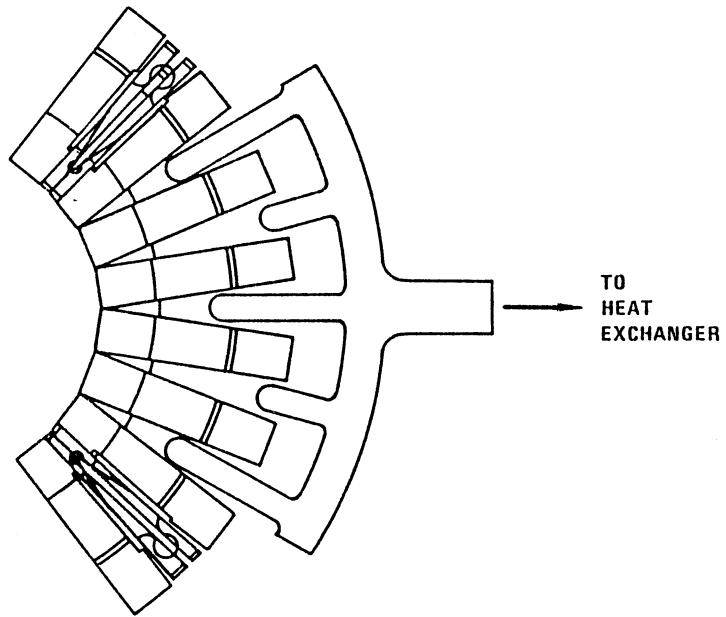
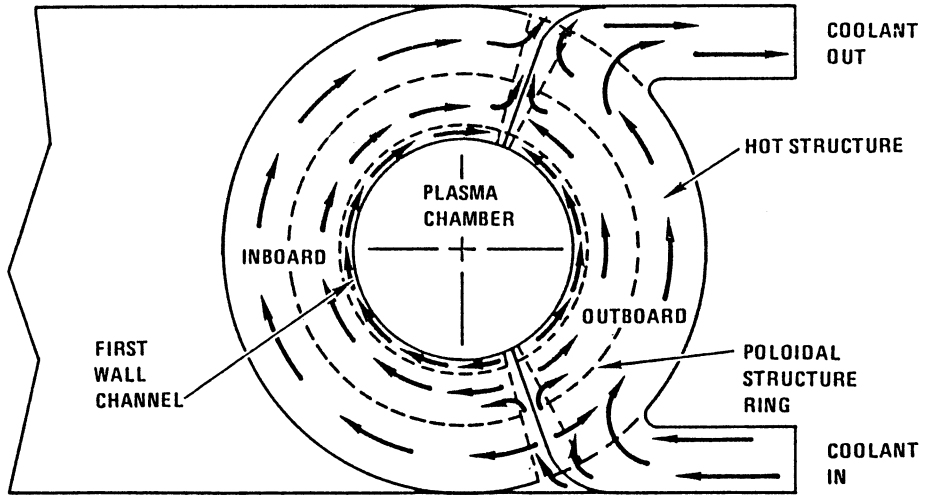


Fig. 1.6.-2a. The aqueous loop-in-pool blanket design.



a. TOP VIEW, DISTRIBUTOR SCHEMATIC



b. SIDE VIEW, INBOARD / OUTBOARD MODULES

Fig. 1.6.-2b. The coolant flow paths in the aqueous loop-in-pool blanket design.

TABLE 1.6.-III
DESIGN CHARACTERISTICS OF THE AQUEOUS BLANKET DESIGN

Major radius (m)	3.9
Minor first wall radius (m)	0.65
Neutron wall loading (MW/m^2)	20.0
Surface heat loading (MW/m^2)	5.0
Thermal power (MW)	2,948.
Net electric power (MW)	1,000.
Tritium breeder	LiNO_2 or LiNO_3
Neutron multiplier	Be
Tritium breeding ratio	1.25
Blanket energy multiplication	1.39
Coolant	water at 15.8 MPa
Inlet temperature ($^{\circ}\text{C}$)	291.
Outlet temperature ($^{\circ}\text{C}$)	326.
First wall material	Cu-Al25
Structural material	PCA or HT-9
First wall thickness (mm)	1.5
First wall temperature, peak ($^{\circ}\text{C}$)	425.
Gross thermal efficiency	35%

neutron wall loading of $20 \text{ MW}/\text{m}^2$). The structural material in the first wall is a high strength copper alloy, Cu-25Al (Cu-0.25% Al_2O_3) and is mechanically attached to a PCA support structure within the blanket.

One of the attractive features of this FPC is the surrounding pool of low-pressure, low-temperature water. If a leak occurs anywhere in the primary loop, the release of tritiated steam will be instantly condensed by the cold pool. If the entire primary loop inventory of hot, tritiated water were mixed with the cold pool, the resulting pool temperature would be $\sim 50^{\circ}\text{C}$. Tritium containment will also be enhanced if the HTO and T_2O remain in the liquid state. Since the torus is submerged in the pool, the FPC will remain covered with coolant in the event of a primary pipe rupture, and will act as a heat sink for decay heat removal. This concept will be subject to detailed study in the design phase.

1.6.3. FLiBe Pool Blanket Design

The pool concept differs from the loop-in-pool concept in that no high-pressure loop is required. The concept is similar to the French Phénix and Superphénix fast (fission) breeder reactor designs in which the primary pumps and IHXs are all contained within the pool. The first wall/vacuum vessel assembly is supported in a low pressure pool of FLiBe [42]. Figure 1.6.-3 illustrates the FLiBe pool configured for the TITAN reactor. The minimum amount of structure between the plasma and the FLiBe enables the reactor to meet the

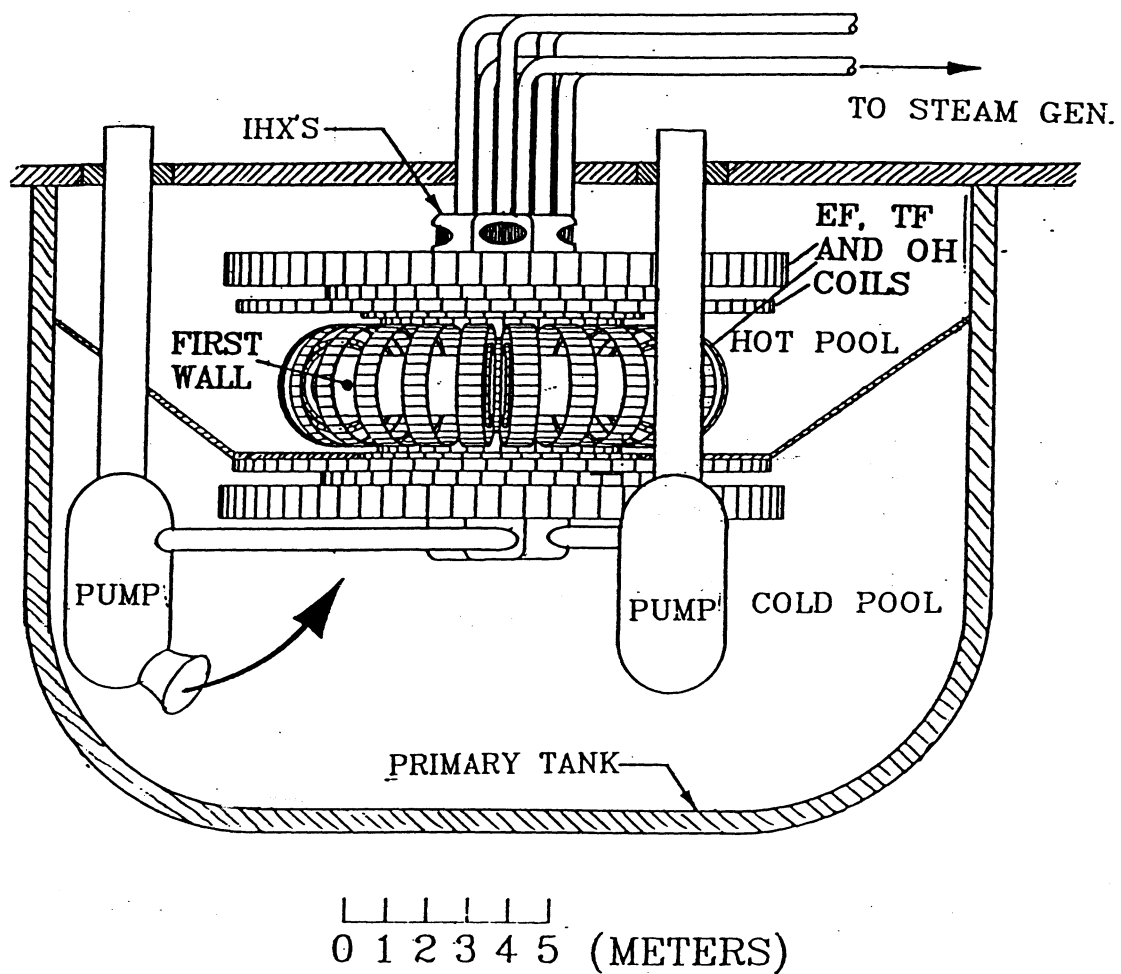


Fig. 1.6.-3. General layout of the FLiBe pool concept.

1-D neutronics requirement of $TBR = 1.2$. Because the FLiBe has a low electrical conductivity MHD or eddy-current effects are not expected.

The first-wall cooling is an inherent problem associated with the pool configuration, since it is difficult to force the coolant towards the first wall in such an open geometry. A baffled first wall can be used to enhance the first wall cooling. In such a configuration the FLiBe first-wall coolant flows through an array of orifices to allow preferential flow to the first wall. With such a configuration, the FLiBe-pool first wall could handle a surface heat flux of about 1.3 MW/m^2 , which corresponds to f_{RAD} of about 0.3 at a neutron wall loading of 20 MW/m^2 ; the divertors in this design are required to handle a significant heat load ($> 10 \text{ MW/m}^2$).

1.6.4. Helium-Cooled Ceramic Design (FISC)

The Fusion Inherently Safe Ceramic (FISC) design [43] uses only low-activation materials, which exhibit only a low level of short-lived activation. The unique idea of the FISC is to place the entire FPC and high-pressure helium primary heat-transport loop inside a prestressed concrete reactor vessel (PCRVR) filled with pressurized helium, as shown in Fig. 1.6.-4. Typical operating parameters for the FISC design are summarized in Table 1.6.-IV. This places the first wall torus under a compressive load. Furthermore, it places the entire primary loop under the same compressive load that balances the tensile load

TABLE 1.6.-IV
DESIGN CHARACTERISTICS OF FISC DESIGN

Major radius (m)	3.9
Minor first wall radius (m)	0.65
Neutron wall loading (MW/m^2)	20.0
Surface heat loading (MW/m^2)	1.5
Thermal power (MW)	2,351.
Net electric power (MW)	1,000.
Tritium breeder	Solid breeder
Neutron multiplier	BeO
Tritium breeding ratio	1.17
Blanket energy multiplication	1.20
Coolant	Helium at 5 MPa
Inlet temperature ($^{\circ}\text{C}$)	540.
Outlet temperature ($^{\circ}\text{C}$)	800.
First wall material	SiC
Structural material	SiC
First wall thickness (mm)	1.9 to 2.5
First wall temperature, peak ($^{\circ}\text{C}$)	1,198.
Power conversion system thermal efficiency	40%

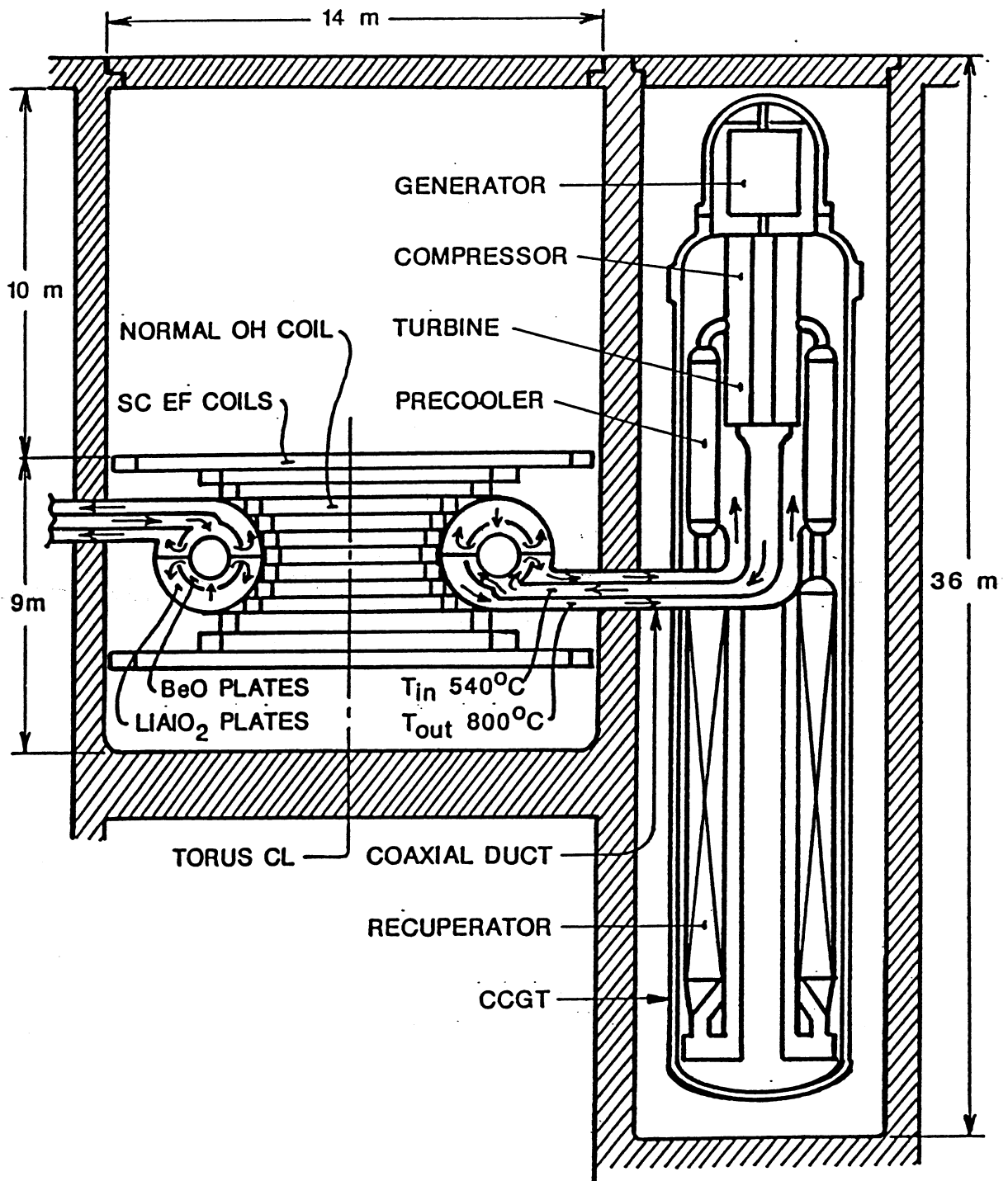


Fig. 1.6.-4a. The TITAN helium-cooled ceramic (FISC) design.

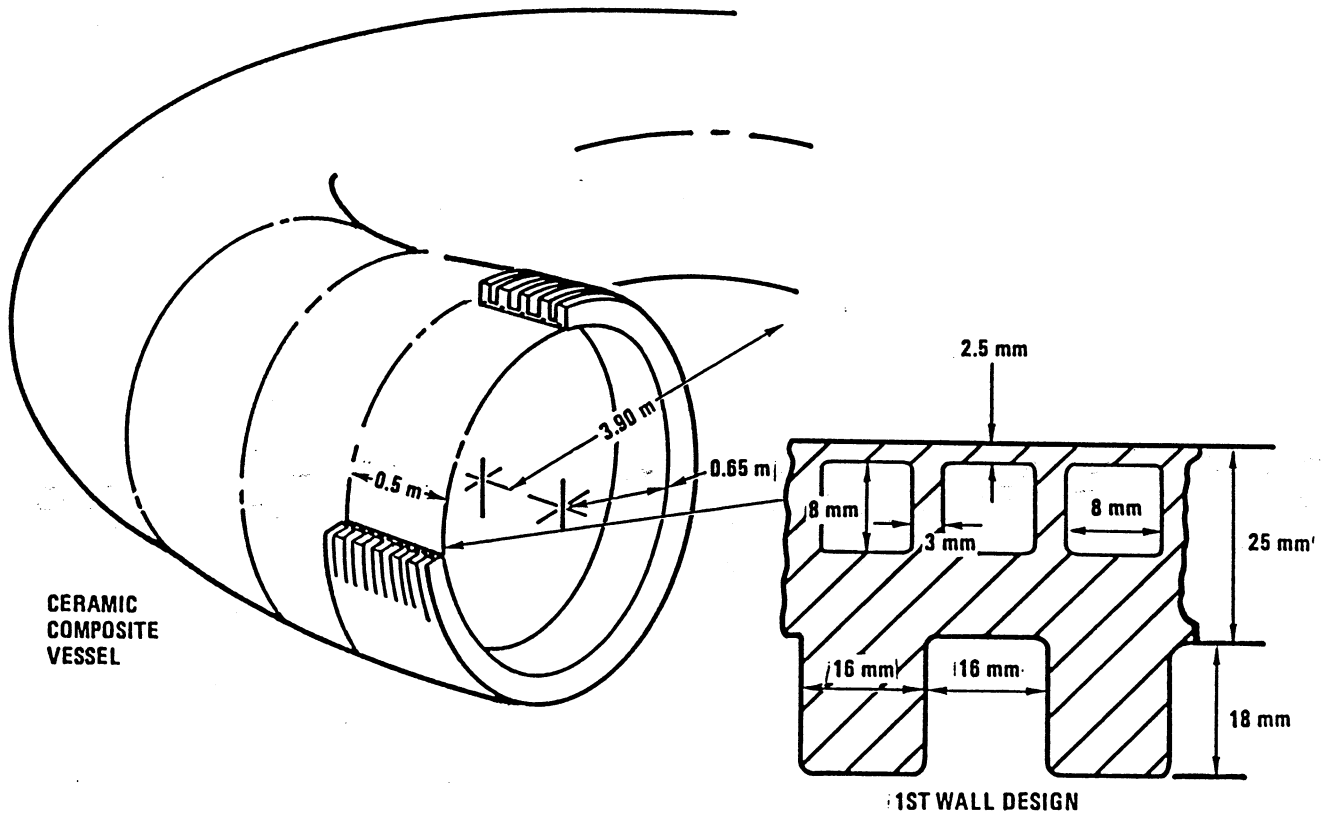


Fig. 1.6.-4b. The ceramic first wall of the TITAN helium-cooled ceramic (FISC) design, which is compressively-loaded.

created by the high pressure, high temperature helium coolant. The result is a ceramic design with only compressive primary stresses.

A closed-cycle, gas turbine power conversion system is located inside the PCRV. High temperature operation is possible with a helium outlet temperature of 800 °C and the power conversion efficiency of about 40%. As with the FLiBe-pool design, there are limitations on first-wall cooling. The surface heat flux limit is roughly 1.5 MW/m^2 , corresponding to $f_{\text{RAD}} = 0.35$ at neutron wall loading of 20 MW/m^2 ; again the divertors in this design are required to handle a significant heat flux.

1.7. MAINTENANCE APPROACH

A potential advantage of high mass power density systems is the feasibility of single-piece maintenance for these systems and possible improvements in the plant availability. Specifically, single-piece FPC maintenance of a totally operational and pre-checked FPC may be possible above a power-density or below a total FPC mass threshold. Above this threshold, more than a single piece would be removed, ranging from few-piece maintenance to fully modular maintenance. The power density corresponding to the minimum-COE design (Table 1.3.-I) may shift once these issues are quantified into an availability model that is more elaborate than used so far. Single-piece maintenance of the FPC is expected to reduce maintenance time and risk and to increase reliability relative to the modular approach. The estimate of time-reduction is based on the elimination of component fit-up and sealing in an activated assembly. These operations can be performed on the replacement FPC in the shop prior to FPC replacement while the plant is generating power. The financial risk associated with remote operations is also reduced with the single-piece approach. Complex maintenance procedures can result in extended outages, particularly if FPC parts have been deformed, while the single-piece approach establishes a limit on the time required to recover from any failure (the time to replace an expended FPC in toto with one that has undergone full non-nuclear testing in conditions that can be more severe, other than radiation, than those encountered in actual nuclear service). An improvement in reliability is achieved by the complete assembly and testing of the FPC prior to installation. The combined improvements in reliability and maintainability can result in improved plant availability.

A major goal of the TITAN study is to quantify the expected availability advantage of the compact reactor approach using single-piece maintenance.

Scheduled maintenance for the balance of plant alone is estimated to require an annual shut-down of 25 days. Typical unplanned outage periods are 50-60 days/year for existing large U.S. plants and this value is also adopted by fusion reactor studies. For discussion, a typical plant with an aggressive availability goal is assumed to require 40 days/year for planned maintenance and 60 days/year for forced outages, resulting in overall availability of 73%. There is a considerable incentive to design a fusion system that can be maintained in an annual shutdown of 25 days, and this goal appears to be credible in the scoping phase for single-piece maintenance [3,6]. The reduction in unscheduled maintenance time, because of FPC pre-testing, and the upper limit on single failure downtime, cannot be quantified without the development of an integrated design and associated equipment specification. If a reduction from 60 to 40 days were achievable, corresponding to a scheduled outage reduction from 40 to 25 days, then the availability would increase from 73% to 82%. This reduction in availability of approximately 10% is a major motivation for further development of the single-piece maintenance approach.

Single-piece maintenance requires that the size and mass of the replaceable unit allow routine transport within the reactor cell and maintenance areas. The heaviest single piece considered in conceptual tokamak designs is the TF coil, and reactor cell crane capacities of 600 tonne are specified by STARFIRE [9]. This value is several times the capacity of standard cranes, but the larger cranes can be supplied at a cost of about 5 M\$. An upper limit on crane capacity will be determined by economic trade studies, considering the building space and structural requirements, as well as the crane cost. The trade studies must also consider special horizontal transporters for the heavier components, and lifts on the order of 1000 tonnes can be performed with gantry cranes. For guidance during the scoping phase, the mass at which single-piece maintenance may become unattractive is assumed to be about 500 tonnes.

A general plant arrangement was developed that takes advantage of the simplicity of the single-piece maintenance approach. A central reactor building containing an enclosed reactor cell connects the shop area at one end to the hot cells and waste processing areas at the other. A straight-through process is envisioned for the FPC replacement, in which the expended FPC is taken to the hot cell for disassembly, and the complete new FPC is brought in from the shop. The intent is to minimize the operations that require the re-assembly of activated or contaminated parts. This approach is expected to simplify the

remote maintenance equipment, since the only operations required in the reactor cell deal with making and breaking of external connections.

The TITAN study scoping phase considered a broad range of blanket and coolant options, rather than aiming at a complete integrated design. The general issues of the definition of the FPC compatible with the maintenance approach and the PF coil structural design were addressed during this phase. The PF coils of the RFP are massive, designed for the life of the plant, and not connected to the rest of the FPC, so they are not considered to be a part of the replaceable FPC. The TITAN study has considered configurations using an "open" PF coil set, but some of the OH coils must be removed or relocated before the replaceable FPC can be removed (Fig. 1.3.-2).

In the CRFPR study [3,6], the replaceable FPC weight (first wall, blanket, shield and TFCs, but not PFCs) is 300 tonnes and is removed as a unit. The blanket breeder, coolant, and part shield is PbLi. The PbLi blanket, which is unique in its large drainable mass and good reflecting/shielding properties, was not selected as an option in the TITAN scoping phase. The preliminary shield specified for the lithium blanket option weighs about 400 tonnes more than that of the PbLi design. The total removable FPC mass (not including PFCs) is greater than 600 tonnes; separation of at least part of the shield from the rest of the FPC may be preferred to single-piece removal. For designs with a lower wall loading, the FPC weight can become so large (e.g., FPC weights over 1000 tonnes for 10 MW/m^2 case) that partitioning of the shield must be considered. The split-shield design would be simplified if the integrated blanket coil concept is used, so that separate TF coils do not need to be removed to gain access to the shield. Detailed design of the service connections and of the structural supports will be required to determine whether the advantages of single-piece maintenance can be retained with a split-shield design.

1.8. CONCLUSIONS OF THE SCOPING PHASE

During the scoping phase, the TITAN design team has succeeded in its interim objectives: to define the parameter space for a high mass power density (MPD) RFP reactor; to explore a variety of approaches to the design of major subsystems; to narrow to two major design approaches consistent with high MPD and low COE; and to reach an intermediate stage which includes preliminary engineering design and integration. The program has retained a balance in its

approach to investigating high MPD systems. On the one hand, parametric investigations of both subsystems and overall system performance are performed. On the other hand, more detailed analysis and engineering design and integration are performed, appropriate to determining the technical feasibility of the high MPD approach to RFP fusion reactors. Because of this balance between parametric system studies and detailed subsystem design, we have come to refer to the TITAN effort as a "PARAPOINT" study.

Detailed technical conclusions are given in individual sections. The physics issues for compact RFP reactors are discussed separately in Sec. 4.8. Major technical results at this interim stage can be summarized as follows:

1. Parametric systems studies continue to suggest a shallow minimum in cost of electricity (COE) versus neutron wall loading, extending from about 10 MW/m^2 to 20 MW/m^2 with the minimum COE at 18 MW/m^2 . Reversed-field pinch reactors in this range have MPD values well in excess of 100 kWe/tonne. The TITAN reference design at a neutron wall loading of 18 MW/m^2 has a MPD of 640 kWe/tonne.
2. Reversed-field pinch systems with high MPD at $15\text{--}20 \text{ MW/m}^2$ neutron wall loading are physically compact systems. The cost of the FPC is a small fraction of plant cost ($< 10\%$), which means that small units can be used to minimize the cost of a development program.
3. Single-piece maintenance of the entire reactor torus (first wall, blanket, divertor sections, with or without the shield) is feasible for high MPD systems. At 18 MW/m^2 neutron wall loading, the entire reactor torus, drained of coolant, can be vertically lifted with a crane and replaced with a complete and pre-tested unit with a minimum amount of down time and start-up time. The full impact of single-piece maintenance and the ability to pre-test the entire reactor torus as a unit on reliability and availability is not yet determined. The shallow minimum in COE largely results from the assumption that the availability is not a strong function of neutron wall load, wall lifetime, and of the maintenance concept, at least at the level of single-piece versus modular approach to design and testing.

4. Reversed-field pinch experiments appear to operate well even when the dominant core plasma loss mechanism is radiation rather than conductive energy transport. This is particularly advantageous for high wall loading systems, as it distributes the plasma energy loss uniformly on the walls. For TITAN, this approach has been adopted, along with four toroidal field divertors as the particle removal system.
5. The dominance of the poloidal field and the relatively high beta make the RFP particularly well suited to liquid-metal cooling. One design approach being pursued uses liquid lithium as coolant and breeder, and vanadium alloy (V-3Ti-1Si) as the structural material. The first-wall, blanket, shield, and divertor cooling are accomplished using lithium throughout this design. No other coolant is needed except for the magnets. This simplifies system integration and design. At 18 MW/m^2 neutron wall loading, the fluid pressure in the first-wall tubes is estimated to be about 10 MPa, but this level is reasonable since the stresses and pumping power requirements associated with this high pressure are modest. The coolant pressure in the blanket is much lower at about two MPa.
6. The integrated blanket-coil concept (IBC) is significantly better suited to the RFP than to the tokamak concept. This is largely due to the lower value of the magnetic field that the coil must produce. The IBC is especially advantageous, perhaps uniquely so, for use as the main divertor field coil in an RFP. The IBC can also be used to generate the toroidal field. In TITAN, the IBC has been adopted for both divertor and TF coils, in order to examine this innovation in depth. In the former case, it truly improves the RFP as a reactor. In the case of IBC as a TF coil, the advantages over a copper TF coil system are less clear. Since the copper TF coil approach appears certain to work, the TITAN study has also chosen to pursue the TF IBC approach.
7. The aqueous loop-in-pool blanket has emerged as an alternative for high-MPD RFP systems. This design incorporates a water-cooled copper first wall and steel structural material for blanket and shield. The cooling is achieved with a loop design, while the FPC as a whole is submerged in a low-pressure water pool to achieve a high level of passive safety. Tritium breeding is achieved using a lithium salt dissolved in the water, while controlling the

pH of the solution to minimize corrosion. Work on this design has been at a less advanced state within the scoping phase, but detailed analysis of this design will commence during the design phase, upon completion of the lithium design.

1.9. DIRECTIONS FOR THE DESIGN PHASE

During the scoping phase of the TITAN study a large number of design concepts and options were considered. Of particular importance are the four blanket concepts reported in Sec. 8. The number of FPC designs to be pursued during the design phase was narrowed to two. This decision was necessary because of inadequate resources to pursue all four designs. The selection of the two concepts to pursue was difficult to make. All four concepts have attractive features. The lithium-loop design promises excellent thermal performance and is one of the main concepts being pursued by the U.S. blanket technology program. The water design promises excellent safety features and use of more developed technologies. The helium-cooled ceramic design offers inherent safety and excellent thermal performance. The molten-salt pool design is the only low-pressure blanket and promises passive safety. In the end, the lithium-loop concept and the aqueous loop-in-pool concept were chosen for detailed conceptual design and evaluation in the design phase of the TITAN study. The choice was made primarily on the capability of each concept to operate at high neutron wall load and high surface heat flux. The choice not to pursue the helium-ceramic and molten-salt designs should in no way denigrate these concepts, since each offers high performance and attractive features when used at lower wall loads; these concepts should be pursued in other design studies.

In the design phase, therefore, the TITAN study will emphasize engineering design and complete technical evaluation of the high-MPD approaches based first on the lithium-loop system and then on the aqueous loop-in-pool concept. Approximately half of the duration of the design phase will be devoted to complete the Li/V design, devoting essentially the full resources of the program. Major efforts will be made to provide the technical material needed to establish engineering feasibility and the design integration. In addition, safety and environmental tasks will receive special attention, and work on the plasma modeling, first wall design, and divertor system will continue. The area

of high-heat-flux components is the most difficult physics-engineering interface.

Once the Li/V design has been brought to a reasonable completion, the TITAN team will concentrate on establishing the feasibility and examining key issues of the aqueous blanket design. All of the major subsystem design and analysis will be addressed along with the assessment of safety and environmental impact. Our philosophy is to establish the technical feasibility and key issues for high-MPD RFP reactors, and having more than one design approach strengthens the case.

Finally, parametric studies will continue so one can better understand the changes in system design in going to lower wall loadings (e.g., about 10 to 12 MW/m²), and in using high-MPD RFP systems in a development program.

REFERENCES

1. R. W. Conn (chairman and editor), "Magnetic Fusion Advisory Committee Panel X Report on High Power Density Fusion systems," (May 8, 1985) and references therein.
2. W. M. Stacey, Jr. (chairman and editor), "Magnetic Fusion Advisory Committee Panel XIII Report on DOE Magnetic Fusion System Studies Program," (Nov., 1985) and references therein.
3. R. L. Hagenon, et al., "Compact Reversed Field Pinch Reactors (CRFPR): Preliminary Engineering Design Considerations ," Los Alamos National Laboratory Report LA-10200-MS (1984).
4. R. A. Krakowski, R. L. Miller, and R. L. Hagenon, "The Need and Prospects for Improved Fusion Reactor," J. of Fusion Energy, 5 (1986) 213.
5. J. Sheffield, et al., "Cost Assessment of a Generic Magnetic Fusion Reactor," Fusion Tech. 9 (1986) 199.
6. C. Copenhaver, R. A. Krakowski, N. M. Schnurr, R. L. Miller, C. G. Bathke, R. L. Hagenon, et al., "Compact Reversed-Field Pinch Reactors (CRFPR): Fusion-Power-Core Integration Study," Los Alamos National Laboratory Report LA-10500-MS (August 1985).
7. R. A. Krakowski, R. L. Hagenon, N. M. Schnurr, C. Copenhaver, C. G. Bathke, R. L. Miller, and M. J. Embrechts, "Compact Reversed-Field Pinch Reactors (CRFPR)," Nuclear Eng. and Design/Fusion 4 (1986)75.
8. B. Badger, et al., "UWMAK-I - A Wisconsin Toroidal Fusion Reactor Design," University of Wisconsin Report UWFDM-68 (1974).
9. C. C. Baker, et al., "STARFIRE - A Commercial Tokamak Fusion Power Plant Study," Argonne National Laboratory Report ANL/FPP-80-1 (1980).

10. B. G. Logan, et al., "MARS: Mirror Advanced Reactor Study," Lawrence Livermore National Laboratory Report UCRL-53480 (1984).
11. D. Steiner, R C. Block, and B. K. Malaviya, "The Integrated Blanket-Coil Concept applied to the Poloidal Field and Blanket Systems of a Tokamak Reactor," Fusion Tech. 7 (1985) 66.
12. H. A. Bodin, R. A. Krakowski, and O. Ortolani, "The Reversed-Field Pinch: from Experiment to Reactor," Fusion Tech. 10, (1986) 307.
13. J. B. Taylor, "Relaxation of Toroidal Plasma and Generation of Reversed Magnetic Fields," Phys. Rev. Lett. 33 (1974) 1139.
14. J. B. Taylor, "Relaxation of Toroidal Discharges," Proc. 3rd Topical Conf. - on Pulsed High-Beta Plasmas, Abingdon (Sept. 1975), Pergamon Press, London (1976) 59.
15. J. B. Taylor, "Relaxation and Magnetic Reconnection in Plasma," Rev. Mod. Phys. 58 (1986) 741.
16. P. Thullen and K. Schoenberg (Eds.), "ZT-H Reversed Field Pinch Experiment Technical Proposal," Los Alamos National Laboratory Report LA-UR-84-2602 (1984) 26-28.
17. M. K. Bevir and J. W. Gray, "Relaxation, Flux Consumption and Quasi Steady State Pinches," Proc. RFP Theory Workshop, Los Alamos, NM (April 28 - May 2, 1980), Los Alamos National Laboratory Report LA-8944-C (January 1982) 176.
18. K. F. Schoenberg, R. F. Gribble, and D. A. Baker, "Oscillating Field Current Drive for Reversed Field Pinch Discharges," J. Appl. Phys. 56 (1984) 2519.
19. K. F. Schoenberg, C. P. Munson, D. A. Baker, R. F. Gribble, R. W. Moses, P. G. Weber, R. A. Nebel, and R. F. Scardovelli, "Oscillating-Field Current Drive Experiments on the ZT-40M RFP," Bull. Am. Phys. Soc. 31 (1986) 1547.

20. A. Buffa, et al., "First Results from the ETA-BETA-II RFP Experiment," Proc. 9th European Conf. on Controlled Fusion and Plasma Phys., Oxford (Sept. 1979), Culham Laboratory (1979) 544.
21. V. Antoni, et al., "Studies on High-Density RFP Plasmas in the ETA-BETA-II Experiment," Proc. 9th Int. Conf. on Plasma Phys. and Controlled Nucl. - Fusion Res., Baltimore, MD (Sept. 1982), IAEA, Vienna, 1 (1983) 619.
22. V. Antoni, et al., "Reversed Field Pinch Plasma with Current Flat-Top in ETA-BETA-II," Proc. 10th Int. Conf. on Plasma Phys. and Controlled Nucl. - Fusion Res., London (Sept. 1984), IAEA, Vienna, 2 (1985) 487.
23. K. Ogawa, et al., "Experimental and Computational Studies of Reversed-Field Pinch on TPE-1R(M)," Proc. 9th Int. Conf. on Plasma Phys. and Controlled Nucl. Fusion Res., Baltimore, MD (Sept. 1982), IAEA, Vienna, 1 (1983) 575.
24. Y. Hirano, T. Shimada, Y. Maejima, K. Ogawa, "Improved Stability Period in High-Current-Density Operation of Reversed-Field Pinch of ETL-TPE-1R(M)," Nucl. Fusion 22 (1982) 1613.
25. D. A. Baker, et al., "Performance of the ZT-40M Reversed-Field Pinch with an Inconel Liner," Proc. 9th Int. Conf. on Plasma Phys. and Controlled Nucl. - Fusion Res., Baltimore, MD (Sept. 1982), IAEA, Vienna, 1 (1983) 587.
26. D. A. Baker, et al., "Experimental and Theoretical Studies of the ZT-40M Reversed-Field Pinch," Proc. 10th Int. Conf. on Plasma Phys. and Controlled Nucl. Fusion Res., London (Sept. 1984), IAEA, Vienna, 2 (1985) 439.
27. R. S. Massey, et al., "Status of the ZT-40M RFP Experimental Program," Proc. 6th Topical Meeting on the Tech. of Fusion Energy, San Francisco (Mar. 1985), Fusion Tech. 8 (1985) 1571.
28. H. A. B. Bodin, et al., Proc. 9th Int. Conf. on Plasma Phys. and Controlled Nucl. Fusion Res., Baltimore, MD (Sept. 1982), IAEA, Vienna, 1 (1983) 641.

29. P. Carolan, et al., "New Results from HBTX1A Reversed Field Pinch," Proc. - 10th Int. Conf. on Plasma Phys. and Controlled Nucl. Fusion Res., London (Sept. 1984), IAEA, Vienna, 2, (1985) 449.
30. T. Tamano, et al., "Pinch Experiments in OHTE," Proc. 9th Int. Conf. on Plasma Phys. and Controlled Nucl. Fusion Res., Baltimore, MD (Sept. 1982), IAEA, Vienna, 1 (1983) 609.
31. T. Tamano, et al., "High Current, High Beta Toroidal Pinch Experiments in OHTE," Proc. 10th Int. Conf. on Plasma Phys. and Controlled Nucl. Fusion Res., London (Sept. 1984), IAEA, Vienna, 2 (1985) 431.
32. B. Alper, et al., "RFP Confinement Studies in ETA-BETA-II," Proc. 12th European Conf. on Controlled Fusion and Plasma Phys., Budapest (Sept. 1985), European Phys. Soc. 1 (1985) 578.
33. P. G. Weber, et al., "Results from the Los Alamos RFP Experiments," Proc. - 12th European Conf. on Controlled Fusion and Plasma Phys., Budapest (Sept. - 1985), European Physical Soc. 1 (1985) 570.
34. G. Rostagni, et al., "The RFX Project: a Design Review," Proc. of 13th Symp. on Fusion Technology, Varese, Italy, 1 (1984) 189.
35. C. G. Bathke, R. A. Krakowski, and R. L. Miller, "A Comparison Study of Toroidal-Field and Bundle Divertors for a Compact Reversed-Field Pinch Reactor," Fusion Tech. 8 (1985) 1616.
36. J. A. Phillips, L. C. Burkhardt, A. Haberstich, R. B. Howell, J. C. Ingraham, E. M. Little, K. S. Thomas, R. G. Watt, "ZT-40M Current Risetime Study," Los Alamos National Laboratory Report LA-9717-MS (October 1983).
37. M. M. Pickrell, J. A. Phillips, C. J. Buchenauer, T. Cayton, J. N. Downing, A. Haberstich et al., "Evidence for a Poloidal Beta Limit on ZT-40M," Bull. Am. Phys. Soc. 29 (1984) 1403.

38. K. A. Werley, "Stable Alfvén Wave Dynamo Action in the Reversed Field Pinch," Ph.D. Thesis, Nucl. Eng. Program, Univ. of Ill.
39. J. Neuhauser, W. Schneider, R. Wunderlich and K. Lackner, "Modeling of Impurity Flow in the Tokamak Scrape-off Layer", Nucl. Fusion 24 (1984) 39.
40. D. L. Smith et al., Blanket Comparison and Selection Study-Final Report, ANL/FPP-84-1 (1984).
41. D. Steiner, et. al., "A Heavy Water Breeding Blanket," 11th Symposium on Fusion Engineering, Austin, Texas, November 1985.
42. D-K. Sze and J. Brooks, "Aspire - Advanced Safe Pool Immersed Reactor," International Symposium on Fusion Reactor Blanket and Fuel Cycle Technology, Oct. 27-29, 1986. University of Tokyo, Tokai-Mura, Japan.
43. G. R. Hopkins, et. al., "Low Activation Fusion Reactor Design," Fusion Reactor Design and Technology, IAEA-TC-392/33, 1983.